SANDIA REPORT

SAND96–2966 • UC–820
Unlimited Release
Printed December 1996

Characterizing Large Strain Crush Response of Redwood

Steven M. Cramer, John C. Hermanson, Wayne M. McMurtry

Prepared by
Sandia National Laboratories
Albuquerque, New Mexico 87185 and Livermore, California 94550
for the United States Department of Energy
under Contract DE-AC04-94AL85000

Approved for public release; distribution is unlimited.

Issued by Sandia National Laboratories, operated for the United States Department of Energy by Sandia Corporation.

Available to DOE and DOE contractors from
Office of Scientific and Technical Information
PO Box 62
Oak Ridge, TN 37831

Prices available from (615) 576-8401, FTS 626-8401

Available to the public from
National Technical Information Service
US Department of Commerce
5285 Port Royal Rd
Springfield, VA 22161

NTIS price codes
Printed copy: A04
Microfiche copy: A01

SAND 96-2966
TTC-1474
Unlimited Release
Printed December 1996

Distribution
Category UC-820

Characterizing Large Strain Crush Response of Redwood*

Steven M. Cramer and John C. Hermanson
Dept. of Civil and Environmental Engineering
Univ. of Wisconsin-Madison
Madison, WI 53706

Wayne M. McMurtry
Transportation Systems Department
Sandia National Laboratories
Albuquerque, NM 87185-0717

Abstract

Containers for the transportation of hazardous and radioactive materials incorporate redwood in impact limiters. Redwood is an excellent energy absorber, but only the most rudimentary information exists on its crush properties. The objectives of the study were to fill the information gap by collecting triaxial load-deformation data for redwood; to use these data to characterize redwood crush, assess current wood failure theories, provide developments toward a complete stress-strain theory for redwood; and to review the literature on strain-rate effects on redwood crush performance. The load-deformation responses of redwood at temperature conditions corresponding to ambient (70°F), 150°F, and -20°F conditions were measured in approximately 100 confined compression tests for crush levels leading to material densification. Data analysis provided a more complete description of redwood crush performance and a basis for assessing proposed general orthotropic stress-strain relationships for redwood. A review of existing literature indicated that strain-rate effects cause at most a 20 percent increase in crush stress parallel to grain.

* This work was conducted at the University of Wisconsin-Madison in Madison, WI supported by Sandia National Laboratories under Sandia Contract 66-1924 and the US Department of Energy under Contract No. DE-AC04-94 AL85000.

Acknowledgments

The authors gratefully acknowledge Kent McDonald and his colleagues at the USDA Forest Products Lab. for assistance in material conditioning and specimen preparation. The technical assistance provided by John Dreger, Jr. and Anton Vermaak of the Structures and Materials Test Laboratory played a key role in the success of the test program. Assistance during testing was provided by Univ. of Wisconsin students Sharnell Williams and Paul Bakke. Scott Talbot of Canton Lumber, Minneapolis, MN provided assistance in lumber selection and Transport Refrigeration of Madison, Wisconsin provided use of a trailer cooling unit. These contributions are most gratefully acknowledged.

Table of Contents

Appendix A

Figures

Tables

1 Introduction

Containers for the transportation of hazardous and radioactive materials incorporate redwood in impact limiters. Redwood is an excellent energy absorber, but only the most rudimentary information exists on its crush properties. The stress-strain interrelationship for any wood species subject to three-dimensional stresses is largely unknown and wood behavior at both high strains and high strain-rates is known only in general terms. Both stress-strain and crush failure theories have been developed based only on uniaxial load tests. The anisotropy of wood adds an additional complexity to measuring wood response and developing suitable theories to describe it. A long history of wood utilization in the building industry has led to design procedures and property information related to simple uniaxial loadings that do not inflict damage to the wood. This lack of knowledge may be surprising for a material that has a long history of engineered use, but the result is difficulty in utilizing wood in more sophisticated designs such as impact limiters.

Two approaches have been used in the past 30 years to model the stress-strain response of wood[1]. The first approach directly models the cellular wood microstructure with various types of isotropic elements. This type of approach has been examined from several research perspectives, but has never been widely applied. The second and more common approach is to assume wood material is a continuum and to apply the principles of orthotropic linear, elasticity (Hooke's Law). It is widely accepted that the assumptions of orthotropy and continuum are approximations for wood. Never-the-less, this approach has been repeatedly adopted without substantial verification for at least 80 years.

No constitutive theory exists for wood materials stressed beyond the linear stress-strain response range; thus **no stress-strain or failure model is available for designing for wood crush in impact limiters**. Different failure models of theoretical or empirical origins have been developed over the years to identify stress states at the onset of crush failure, but no theory has even been proposed to compute stress-strain states past the linear and assumed elastic range. The interactions of multiaxial stresses beyond material linearity are completely unknown.

The objectives of this research program were to:

1. collect triaxial load-deformation data for redwood,
2. analyze the collected crush data so that the authors could:
   a) assess the ability of available crush and failure models to accurately predict wood performance,
   b) provide developments toward establishing a large-deformation stress-strain model for redwood,
3. review the state-of-the-art on strain rate effects on wood crush performance.

Triaxial tests of 4 inch redwood cubes were conducted at ambient (approximately 70°F), 150° F and -20° F conditions. These conditions will be called *ambient*, *hot*, and *cold* conditions respectively throughout this report. The tests consisted of applying vertical load to each redwood cube confined in an instrumented, steel box. The load was applied using two

displacement rates, one to capture linear behavior and one for the crush range. Loads were applied to the onset of densification. Lateral loads and deformations resulting from the restrained lateral expansion of the redwood cube were measured. General fiber (grain) orientation with respect to the applied vertical load was controlled and varied from 0 to 90 degrees in predetermined increments.

Specimens were prepared according to a developed procedure[2] such that a minimum of 4 replicates had the same target grain orientation with respect to the active loading direction. Figure 1 shows the material axes system for wood. The longitudinal direction corresponds to the parallel-to-grain direction and the radial and tangential directions correspond to perpendicular-to-grain directions. The redwood specimens consisted of 4 inch cubes in which the grain orientation was targeted to a value between 0 and 90 degrees as shown in Table 1. A minimum of 4 replicates were required by the test procedure and in several cases five replicates were tested.

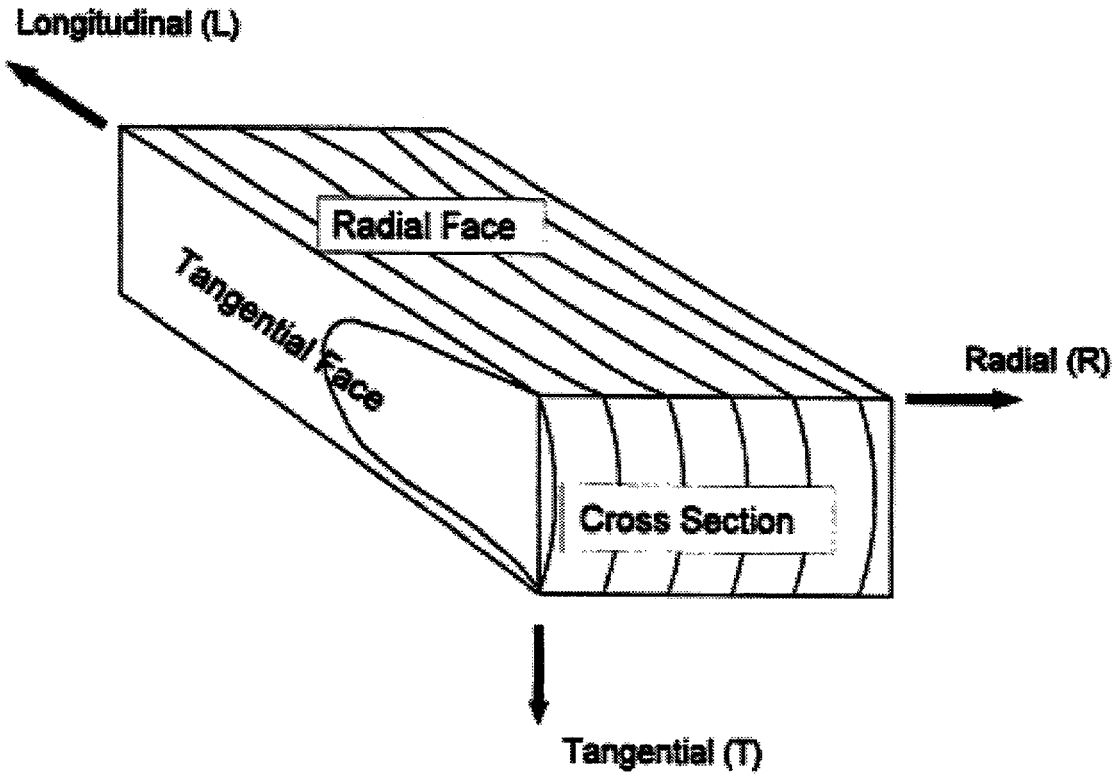

Figure 1. Radial, Tangential, and Longitudinal Axes System for Wood Materials

Table 1. Replicates Tested for Target Grain Angles

Target Surface Grain Angle degrees	Ambient Condition Test Specimens	150° F Test Specimens	-20° F Test Specimens
0	5	5	4
5 - T Face	5	4	4
10 - T Face	4	4	4
30 - T Face	4	4	4
90	4	4	6
5 - R Face	4	4	4
10 - R Face	5	4	4
30 - R Face	5	4	4
Tests Conducted=>	36	33	34

Each test consisted of application of vertical load on a 4-inch redwood cube confined by very rigid side plates of steel. The vertical load was applied at two quasi-static displacement rates of 0.014 inches per minute for the first 10 minutes of the test and 0.263 inches per minute thereafter until the onset of material densification. As shown in the cut-away view in Fig. 2, the side plates of steel were restrained from movement by a 24-inch steel ring that encompassed the wood cube and side plates. The side plates were instrumented such that the expansion and resultant lateral loads were measured. The complete test device was placed in a convection oven for the hot tests and a freezer for the cold tests. The test specimens were conditioned to a uniform moisture content of approximately 14% before testing, but no special humidity controls were employed within the test chamber.

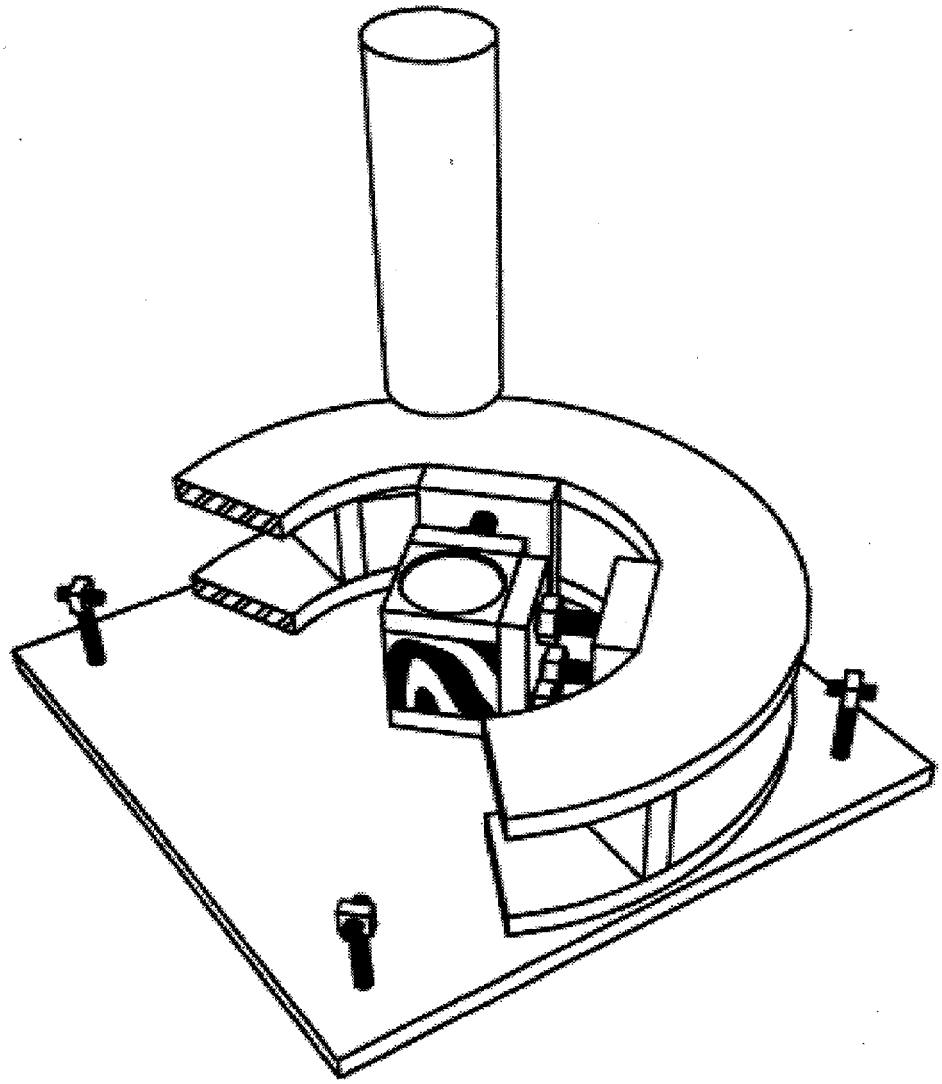

Figure 2. Triaxial Redwood Test Device

2 Parameters That Influence Redwood Crush

This study has examined several key properties that are known to influence the crush behavior of redwood. These properties are identified and defined here.

Specific Gravity (SG): Specific gravity is the mass of the oven dry redwood cube divided by the mass of water occupying the original, undeformed volume at the time of the test. This property is widely used as a general index of wood quality and other wood properties. Use of specific gravity is preferred in this study over density because density combines both moisture content and specific gravity. It was not feasible to obtain nearly 100 test specimens with the same specific gravity. Therefore, specific gravity was allowed to vary. Specific gravity for the redwood tested in this study was measured and ranged from 0.29 to 0.45.

Growth Rings per Inch (Rings): The number of growth rings per inch was measured and found to have a significant correlation with specific gravity ($r^2 = 0.75$). Although growth ring count is not always a reliable indicator of specific gravity, we hypothesized that the number of growth rings per inch in some situations may be a better predictor of crush behavior than specific gravity because growth ring count better reflects the actual differences in specimen microstructure within the redwood species than specific gravity. For two specimens with like specific gravities and moisture and temperature conditions, our data shows the one with a greater number of rings per inch will have a higher crush strength. Ring count ranged from 2 to 24 growth rings per inch.

Grain angle (θ, γ, ϕ): The angle between load application and grain direction is known to strongly influence mechanical behavior of wood specimens because of the assumed orthotropy of the material. This was a primary variable in the test program as indicated in Table 1. Grain angles were measured as previously described[3] on each side-grain surface of the cubical wood specimens and represent the general orientation of individual wood fibers. Surface angles were defined as Theta and Gamma, with Theta corresponding to the angle on the 1-3 face and Gamma to the 2-3 face. These surface angles represent components of the three-dimensional grain angle called Phi. Figure 3 shows the surface and space angles on a typical redwood specimen. The angle of the growth rings on the surfaces (not shown in Fig. 3) must be considered in addition to the surface angles to establish the radial and tangential directions.

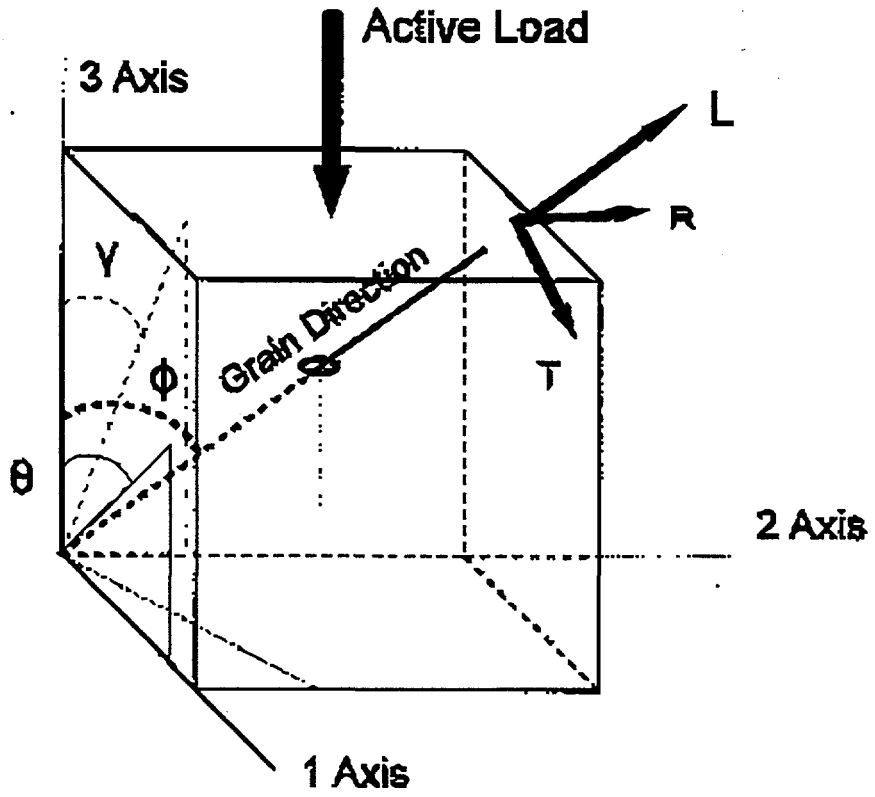

Figure 3. Surface Angles,θ and γ, and Space Angle, ϕ, Representing the Grain Angle

Temperature and Moisture Content: Mechanical properties of wood are strongly influenced by both temperature and moisture content (MC), but in application the two conditions are often interrelated. The combination of relative humidity and temperature determines the equilibrium moisture content of the wood and, in practice, relative humidity usually changes with temperature. In general, the mechanical properties of wood decrease when heated and increase when cooled[4]. These changes are diminished as the wood approaches 0 percent moisture content. Temperature-induced changes in mechanical properties are considered reversible below 210° F (100° C). At +120° F (+50° C), uniaxial compressive strength decreases by 10 percent at 0 percent MC and between 12 and 45 percent MC, the decrease is 25 percent[2] At -58° F (-50° C) the increases are 20 and 50 percent for 0 percent and 12 to 45 percent MC respectively[4].

As indicated in Table 1, three temperature conditions were included in the investigation. Ambient conditions consisted of room temperatures varying in the range of 68 to 72°F. For both hot (150°F) and cold (-20°F) tests, specimens were subjected to approximately 24 hours of conditioning to achieve constant temperature conditions throughout the specimen. The target temperatures were then maintained throughout the test by active heating and cooling.

All specimens were equilibrated to approximately 13 percent moisture content before testing, but

relative humidity was not controlled during testing. As expected, substantial drying of the specimens occurred at the 150° F exposure. At -20° F there were not noticeable changes in moisture content from the ambient conditions. In this case, the moisture freezes and is locked in the specimen before any significant change in moisture content can occur.

Lateral Restraint: As the wood specimens were compressed, they attempted to expand laterally. Expansion was restrained by the stiff steel test device ring that encircled the test specimen and steel plates positioned on the sides of the specimens. The resulting confinement induced triaxial stresses within the wood specimens.

Test Dependent Factors: Several factors are known to influence the results in a confined compressive test of this type. Friction forces will occur on all surfaces where the wood and steel surfaces meet. These friction forces, particularly on the lateral surfaces, will have some influence on the load-deformation response of the specimen and the measured crush load. Microscopic and macroscopic material asperities on all surfaces of the specimens influence the measured deformations[5] Unfortunately, little has been published from previous test programs on quantifying these factors suggesting that they were not considered. As load rate increases, it is generally recognized that load-deformation response and crush properties may increase. Our test results provided evidence that load rate will influence the crush properties of redwood.

3 Crush Strength and Specific Energy Parallel to Grain - New Data Compared to Data From Previous Investigations

3.1 Definitions

Investigations by Hill and Joseph[6,7] and Von Riesemann and Guess[8] have reported average crush strength and specific energy values for various tests of redwood. These parameters have been sometimes defined differently. Key definitions are presented below.

Nominal Values: Nominal values are those that are not corrected for end and lateral restraint effects. These values are presented here for comparison to those published by other investigators. Later, we examine the potential significance of the wood-metal interfaces.

Nominal Crush Strength: Hill and Joseph defined crush strength as the cumulative average force divided by the original area[6]. The cumulative average force was computed as the area under the load deformation curve divided by the deflection. Von Riesemann and Guess identified both peak crushing stress and cumulative average. The average crush stress was defined as the area under the load-deflection diagram divided by the limiting deflection. The limiting deflection or crush state is the "bottoming point" which corresponds to the deflection just at the onset of material lock-up. When comparing our data to those of other investigators, we employed the original investigator's definition of crush strength. Later in this report, the nominal average crush strength is defined to be the average applied stress the specimen can resist between 10 and 40 percent crush. The 10 to 40 percent volumetric crush range was in the crush plateau for all specimens tested. This new definition is needed because a clearly defined bottoming point is not exhibited at high grain angles.

Nominal Static Specific Energy: This parameter is defined as the energy absorbed per pound of material being crushed. The bottoming point is used as a limiting deflection.

3.2 Average Nominal Crush Strength and Specific Energy - Previous Studies and New Data

Hill and Joseph collected some of the first data on crush behavior of wood[6,7]. Table 2 shows some of their data and the new data in a comparable format. Percent crush for the UW data is based on volumetric crush which is nearly equal to percent crush based on the active deflection only. Although the specific gravities in each study were comparable, there was a 3 percent difference in moisture content. Joseph and Hill used a loading rate of approximately 2 inches of displacement per minute, whereas in the current study, rates of 0.014 inches for 10 minutes and 0.263 inches/min. thereafter, were used. The UW parallel-to-grain results are consistently 28% less than those of Joseph and Hill, and this difference is consistent with the known potential effect of loading rate and the difference in specimen moisture contents[4]. General agreement of test values is obtained when these corrections are applied. The UW perpendicular-to-grain results at 20 percent volumetric crush are over 30 percent higher than those of Joseph and Hill. This

difference is diminished as 60 percent crush is approached. The variability of crush strength results in each study was comparable. The comparison of specific energy between the two studies is similar to the crush strength comparison. These values are shown in Table 3.

Table 2. Crush Strength Results of Joseph and Hill[5] and the Univ. of Wisc. Study

Crush Direction	Percent Crush	Joseph and Hill[5] Results			Univ. of Wisconsin Results		
		Cumulative Avg. Crush Strength, psi		Std. Deviation, psi	Cumulative Avg. Crush Strength, psi		Std. Deviation, psi
Parallel to grain	20	Avg. SG » 0.33 Avg. MC » 10%	5,070	810	Avg. SG = 0.32 Avg. MC = 13%	3,640	660
	40		5,350	860		3,850	740
	60		5,560	920		3,970	820
Perpendicular to grain	20		610	76	Avg. SG = 0.31 Avg. MC = 13%	800	100
	40		790	90		880	110
	60		1,090	230		1,070	180

Von Riesemann and Guess conducted a redwood crush test program that included extreme temperature exposures[8]. These were penetration type tests as opposed to our tests that loaded the complete cross section. Different densities and potentially different moisture contents were used in each study making direct comparison difficult. As shown in Table 4, the greatest difference is crush strength at ambient (70° F) conditions where the UW results are considerably less than those measured by Von Riesemann and Guess. A displacement rate of 0.2 in./min. was used for these tests. This rate was higher than the initial displacement rate and slower than the second displacement rate used in the UW tests. The difference in peak crush strength can not be entirely attributed to differences in displacement rates.

Table 3. Specific Energy Results of Joseph and Hill[5] and the Univ. of Wisc. Study

Crush Direction	Percent Crush	Joseph and Hill[5] Results			Univ. of Wisconsin Results		
		Specific Energy, ft-lb/lb		Std. Deviation, ft-lb/lb	Specific Energy, ft-lb/lb		Std. Deviation, ft-lb/lb
Parallel to grain	20	Avg. SG » 0.33	6,500	530	Avg. SG = 0.32 Avg. MC = 13%	4,810	260
	40		13,640	1280		10,000	580
	60		21,350	2230		15,350	1,010
Perpendicular to grain	20		810	170	Avg. SG = 0.31 Avg. MC = 13%	1,060	160
	40	Avg. MC » 10%	2,070	290		2,330	340
	60		4,410	590		4,190	600

Table 4. Crush Strength and Specific Energy Results of Von Riesemann and Guess[6] and the Univ. of Wisc. Study

Temp., Degree. F	Von Riesemann & Guess[6] Results					
	Sample Size	Density, lb/cu. ft.	Moisture Content, %	Peak Crush Stress, psi	Avg. Crush to Bottoming, psi	Spec. Energy, lb-ft/lb
-32	1	20.6	NA	8,150	6,610	28,600
70	8	21.3	NA	6,120	5,380	22,800
+152	3	22.9	NA	6,650	5,040	19,900
	University of Wisconsin Parallel to Grain Results					
-20	4	26.3	13	7,220	6,720	23,800
70	5	22.4	13	3,900	3,990	17,100
+150	5	23.2	4	6,360	5,650	20,400

Much of the variability in results in this study and previous investigations can be attributed to variations in specific gravity (SG). Figure 4 shows the relationship between specific gravity and maximum crushing strength of green virgin growth redwood tested parallel to grain as gathered by Luxford and Marqwardt[9] and data obtained in this study. The trend of the new data roughly parallels that obtained by Luxford and Markwardt[9].

It is obvious from Fig. 4, as moisture content decreases, crush strength increases. Note that any degrade caused by the 150° F temperature exposure is more than offset by the resulting property

increase caused by decrease in moisture content. The -20° F data shows a clear increase in peak crush strength over that of ambient.

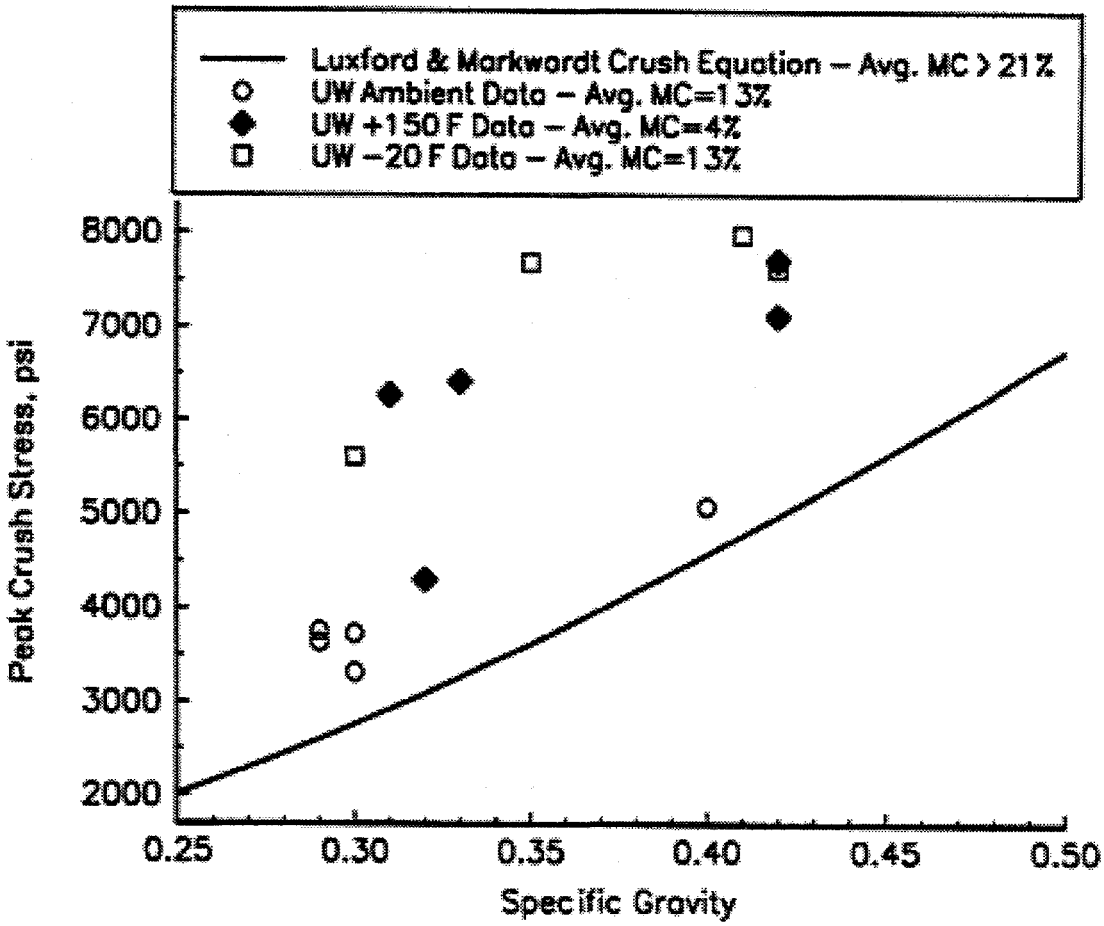

Figure 4. Relationship of Peak Crush Stress to Specific Gravity

4 Correlation of Parameters on Crush Strength

The influence of variations of parameters such as grain angle and specific gravity on crush strength was studied. Crush strength was defined as the average nominal crush strength from 10 to 40 percent volumetric strain as discussed in Section 3. This range is consistent and comparable between specimens at all grain angles, specific gravities and temperatures.

Table 5 shows computed correlation coefficients for different parameters on crush strength for different combinations of data. Low correlation's result from either insufficient variation of the parameter or as a result of a general lack of correlation. Traditional knowledge of wood science suggests that the correlation's of crush strength with MC, angle between load and grain direction (Phi), and temperature (Temp.) should be negative. Crush strength should increase with a decrease in these values. Existing knowledge also suggests the correlation of crush with specific gravity (SG) and growth rings per inch (Rings) should be positive. Strong positive correlation's of crush strength with specific gravity and rings per inch are shown in Table 5 and there is some evidence that the correlation of crush with rings per inch is stronger than with specific gravity. Moisture content correlates well with crush strength primarily in the data set combining ambient and hot data where a significant variation in moisture content occurred. Temperature correlated well with crush strength in the ambient-cold combined data set, but the effect of moisture content overshadowed any influence of temperature in the combined ambient-hot data set. The influence of small grain angle variations within each grain angle target category held no significant correlation with crush strength. The one exception to this occurred in the 90 degree Hot data set, where the correlation was coincidental because the Phi angles were all within one degree. Generally the listed parameters show stronger correlation with crush strength parallel to grain than with crush strength perpendicular to grain.

Table 5. Correlation Coefficients between Crush Strength andother Parameters for Parallel and Perpendicular-to-Grain Data Sets. Shaded Cells Serve to Accentuate the Unshaded, Significant Correlation's.

Data Set	Samples	MC	SG	Rings	Phi	Temp.
0 Degree-Ambient	5	0.27	0.78	0.86	0.17	NA
0 Degree-Hot	5	0.57	0.84	0.97	-0.31	NA
0 Degree-Cold	4	0.03	0.87	0.95	0.47	NA
0 Degree-Amb. & Hot	10	-0.74	0.88	0.89	0.16	0.71
0 Degree-Amb. & Cold	9	0.23	0.85	0.81	-0.11	-0.86
90 Degree-Ambient	4	0.96	0.21	-0.10	0.27	NA
90 Degree-Hot	4	0.02	0.81	0.91	-0.96	NA
90 Degree-Cold	6	0.35	0.55	0.07	-0.52	NA
90 Degree-Amb. & Hot	8	0.40	0.66	0.58	0.19	0.44
90 Degree-Amb. & Cold	10	0.40	0.22	0.15	0.13	-0.79

5 The Effect of Specific Gravity, Moisture Content, and Ring Count on Crush Strength

Figure 5 shows average crush strength for 10 to 40 percent volumetric crush plotted against average grain angle (Phi) for each specimen tested. Considerable variability in crush was experienced because specific gravity, ring count, moisture content and temperature all play a role in addition to the Phi in determining crush strength. These parameters were measured, however, and the measurements provide a basis for more precisely defining the separate effect of grain angle than shown in Fig. 5.

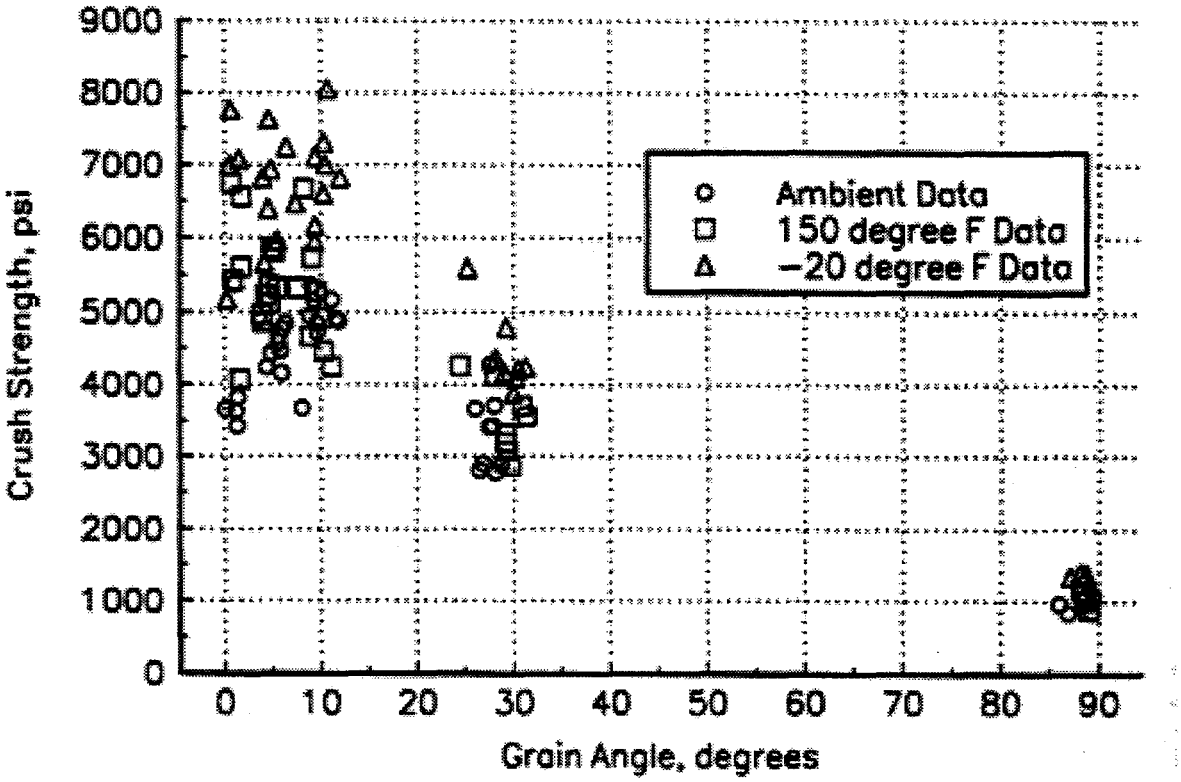

Figure 5. All UW Crush Data Plotted Against Grain Angle (Phi)

The separate influences of specific gravity, temperature, and moisture content on redwood crush stress were found to approximately follow standard adjustments published in the literature for parallel-to-grain compressive strength of several wood species. These adjustments are shown in Table 6. The literature does not contain adjustments for all conditions examined in this test program and thus the literature adjustments were insufficient for adjusting the collected data. Consistent with the data measured in this program, the standard adjustments show that the decrease in crush stress associated with elevated temperature of 150°F is more than offset by an increase associated with drying at elevated temperatures.

From a statistical view point, this study has not provided sufficient data to rigorously define the separate effects of specific gravity, moisture content, and ring count on crush strength to generally characterize all redwood material. However, it is obvious from an examination of the data that strong correlation's with specific gravity, ring count, and moisture content do exist. Knowledge of wood science combined with the data collected provides a basis for proposing relationships that can be used to interpolate and, in some cases, extrapolate these data to common comparison points. Although some of the proposed relationships may be generally valid for all redwood, such uses should be approached with great caution because of the small sample size of data used to form these relationships. The purpose of these equations is to normalize the data collected in this study to standard comparison points. Other equally acceptable means of adjusting the data also exist. The literature-based adjustments in Table 6 are recommended for general use outside the context of this study.

Table 6. Standard Adjustments for Crush Stress Parallel to Grainfor Specific gravity, Moisture Content, and Temperature

Parameter	Adjustment	Source
Specific Gravity	Crushing strength = 14600 $(SG)^{1.04}$	Forest Products Laboratory 1987 [4]
Moisture Content	For each 1% change in MC from 12% adjust crush stress by 5% of room temp. crush stress at 12% MC using the opposite sign. Valid for the range of 0% to 21% moisture content.	Gerhards 1982[10]
Temperature	For 150°F decrease crush stress at room temp. and 12% MC by 30%. For -20°F increase crush stress at room temp. and 12% MC by 40%.	Gerhards 1982[10]

A least-squares regression was conducted to establish coefficients for a linear crush strength relationship within each target grain angle data set that depends on specific gravity, moisture content and ring count. It is well known that strength properties of wood vary between the fiber saturation point and the oven dry condition. Therefore, the difference between fiber saturation point and the actual moisture content was used as a parameter rather than moisture content. The published fiber saturation point of redwood is 21 percent[4]. The equations are all of the form shown in Eq. 1.

$$Crush = A*SG+B*(FSP-MC) +CXRINGS+D \quad (1)$$

Crush = average nominal crush stress from 10 to 40 percent crush, psi,
SG = specific gravity,
FSP = fiber saturation point moisture content (21 percent for redwood), decimal percent,
MC = moisture content of redwood samples, decimal percent,
RINGS = number of growth rings per inch for redwood samples,
A, B, C, D = Empirical coefficients established from regressions with the UW data.
Table 7 lists the number of samples, the coefficients (A, B, C, and D) associated with target grain angle data sets, and the resulting correlation coefficient indicating how well the resulting equation fit the data. Average properties are also shown in Table 7. Although the variations in average properties are small, direct comparisons of average crush strength between these sets would be meaningless without a common basis of comparison.

The cold tests did not contain sufficient variation of several parameters to define meaningful relationships. For these situations, selected parameters were set to zero and least-squares regressions were performed with a reduced number of coefficients. As stated earlier, these regressions are used to adjust crush strength data to common comparison points. Comparison points were chosen near the average condition for each data set tested. Table 8 lists average values of the parameters used in the crush equations. The average values are consistent from data set to data set except for moisture content, which was influenced by test temperature as previously explained.

	Samples	A psi	B psi	C psi-in./rings	D psi	r^2	Avg. MC	Avg. SG	Avg. Crush Strength (psi)	Avg. Phi
0 Degree-Amb. & Hot	10	390	11,603	113.6	2235	0.98	8.5%	0.34	4836	1.2°
5 Degree. R-Amb. & Hot	9	6,701	10,385	0	1146	0.90	8.8%	0.37	4908	5.2°
5 Degree. T-Amb. & Hot	8	2,849	8,771	38.1	2290	0.96	9.2%	0.36	4931	4.7°
10 Degree. R-Amb. & Hot	8	8,428	3,274	79.8	-470	0.70	9.3%	0.41	4992	9.7°
10 Degree. T-Amb. & Hot	9	11,463	11,089	14.2	-890	0.88	9.5%	0.39	4986	9.5°
30 Degree. R-Amb. & Hot	8	0	8,290	35.4	1915	0.82	10.2%	0.38	3265	28.6°
30 Degree. T-Amb. & Hot	9	10,648	5,429	0	-894	0.73	10.3%	0.36	3563	27.8°
90 Degree. Amb. & Hot	8	1486	339	0	447	0.05	8.3%	0.34	989	88.2°
0 Degree-Cold	4	2010	59,667	127.9	-162.7	1.00	13.4%	0.37	6755	0.7°
5 Degree. R-Cold	4	-72,249	90,197	873.8	15,058	1.00	14.1%	0.39	6728	4.8°
5 Degree. T-Cold	4	4,564	45,466	107.9	-121.8	1.00	13.4%	0.36	6550	5.5°
10 Degree. R-Cold	4	-2,415	51,988	209.2	1125	1.00	14.0%	0.39	6793	10.0°
10 Degree. T-Cold	4	6,080	45,645	111.0	-902.8	1.00	13.7%	0.40	6961	10.5°
30 Degree. R-Cold	4	0	11,506	0	3421	0.58	14.8%	0.33	4133	29.4°
30 Degree. T-Cold	4	15,636	0	0	-652	0.99	12.9%	0.34	4714	29.1°
90 Degree. Cold	6	3,265	0	0	244	0.31	13.3%	0.31	1260	88.4°

Table 7. Regression Coefficients for Equation 1.

Table 8. Average Values of Crush Strength Relationship Parameters for Different Data Sets

Data Set	Average/Range of Specific Gravity	Average/Range of Moisture Content	Average/Range of Growth Rings per Inch
All Data	0.37 (0.29-0.45)	11% (2%-16%)	13.3 (2.3-23.8)
Ambient Data	0.37 (0.29-0.45)	14% (13%-14%)	13.6 (2.3-23.8)
150° F Data	0.37 (0.30-0.45)	5% (2%-10%)	13.9 (2.3-23.8)
-20° F Data	0.37 (0.29-0.45)	14% (12%-16%)	12.6 (2.3-22.5)

6 Effect of Grain Angle on Crush Strength

6.1 UW Data Trends and Hankinson's Formula

Compressive strengths of wood at load-to-grain angles between 0 and 90 degrees have long been computed using Hankinson's Formula[11]. This empirical formula is shown in Eq. 2 and offers an interpolation between strength at 0 degrees and strength at 90 degrees. Variations of Hankinson's formula generally consist of different powers on the sine and cosine terms. A power of 2.0 corresponds to the original form and is most widely used. The Wood Handbook[4] recommends a value of 2.5 for wood in compression.

$$\sigma_\phi = \frac{(\sigma_I \sigma_\perp)}{\sigma_I \sin^2(\phi) + \sigma_\perp \cos^2(\phi)} \qquad (2)$$

σ_ϕ = Crush strength at load-to-grain angle, Phi,
$\sigma_|$ = Parallel-to-grain crush strength,
$\sigma_\perp$ = Perpendicular-to-grain crush strength,
ϕ = Angle between direction of load application and grain direction.

Using the relationships presented in Section 5, the data collected in this report were normalized to near-average SG-MC-RINGS properties for the data set. The average nominal crush strength for each target angle group was the plotted against the average grain angle (Phi) for each group. Figure 6 shows the combined ambient and hot data set normalized values plotted against grain angle, Phi. These values were established from Eq. 1 using the parameters listed in Table 7. Ambient/hot redwood specimens where the grain angle occurs on the tangential face consistently display higher crush strength in comparison to the same grain angle occurring on the radial face. Hankinson's formula (Eq. 2) is also plotted in Figure 6 using the parallel-to-grain and perpendicular-to-grain values established from the data relationships. Considering that the endpoint values at 0 degrees and 90 degrees were selected to fit the data, the formula does not provide a good fit to intermediate data.

Normalized ambient crush strengths are compared to corresponding hot and cold values in Fig. 7. Cold data specimens with 5 or 10 degree grain angles on the radial face showed higher increases in average crush strength compared to specimens with grain angles on the tangential face. There was insufficient cold data for 30 degree grain angles on the radial face to establish a representative value for a specific gravity of 0.36. The values for a specific gravity of 0.33 are shown in Figs. 7 and 8 but are lower than would be expected for the standard specific gravity of 0.36.

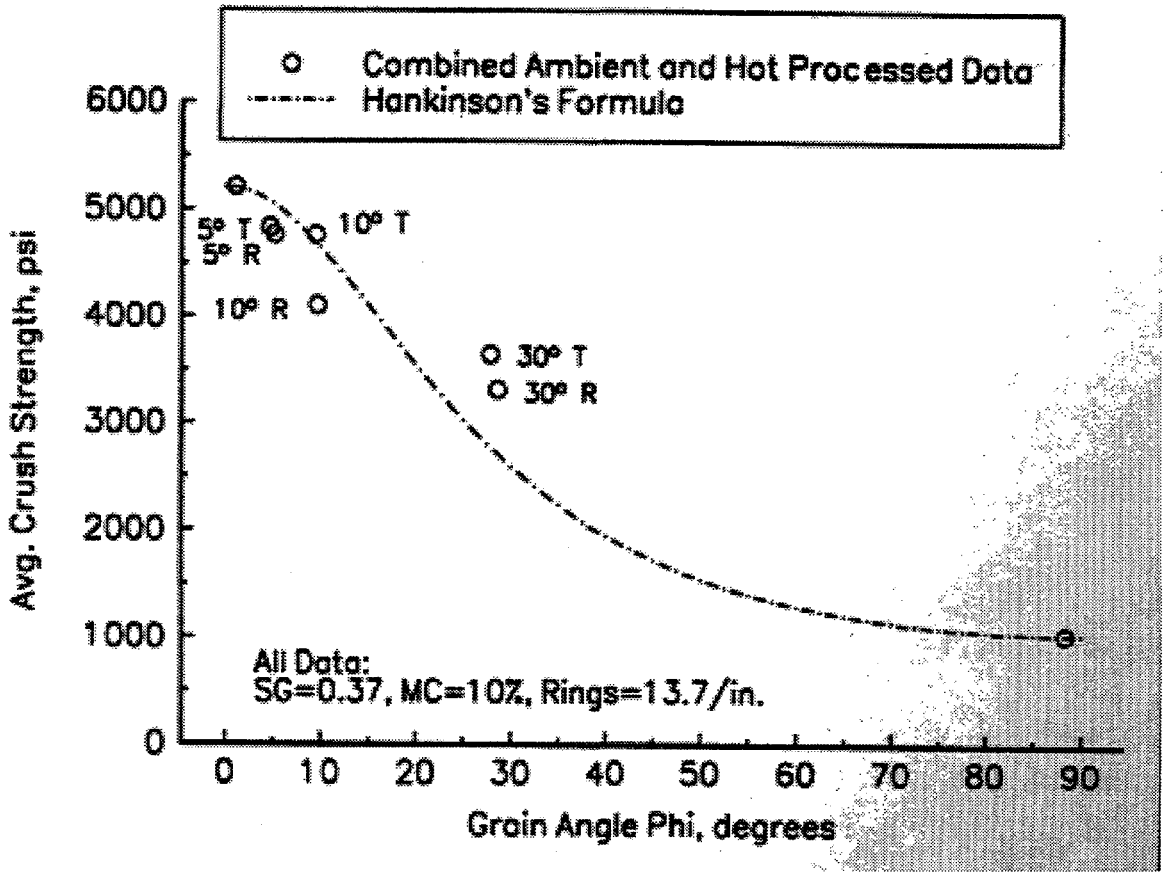

Figure 6. U of W Ambient and Hot Data Adjusted With SG-MC-Rings Relationships and Hankinson's Formula (Eq. 2) Using Parallel-to-Grain and Perpendicular-To-Grain Crush Values from the Plotted Data

Normalized cold data are shown in Figure 8. At Phi of 5 and 10 degrees, specimens with the grain angle on the radial face displayed higher crush strength values compared to the grain angle occurring on the tangential face. The difference was consistent for both 5 and 10 degrees. Of most interest, these normalized values were roughly equal or greater than the normalized crush strength parallel-to-grain (Phi = 0 degrees). Once again, Hankinson's formula is also shown with 0 and 90 degree crush strength values selected to fit the data shown. The formula does not fit the intermediate values, but some improvement in fit is achieved with a power of 2.5.

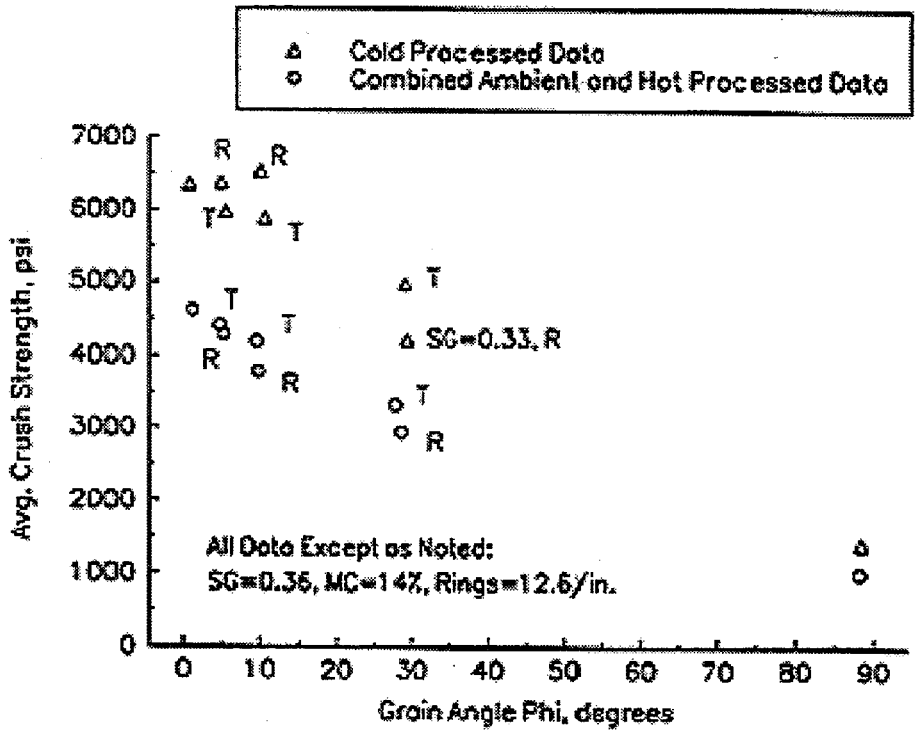

Figure 7. Comparison of Crush Strength Between Processed Ambient-Hot and Cold Data. T = Grain Angle on the Tangential Face. R = Grain Angle on the Radial face

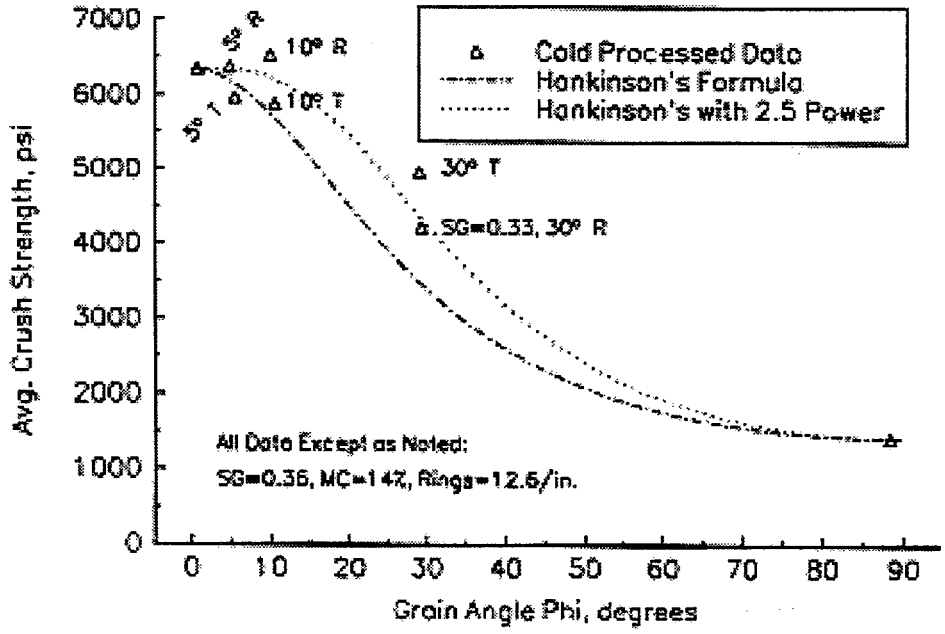

Figure 8. U of W Cold Data Adjusted With SG-MC-Rings Relationships and Hankinson's Formula Using Parallel-to-Grain and Perpendicular-to-Grain Crush Values from the Plotted Data

Table 9 lists average ambient, hot, and cold crush strength data for each target grain angle group. The hot values were 17 percent stronger than the ambient values on average. As explained previously, this indicates that the effect of reduced moisture content more than offset any decrease caused by the heating from ambient to 150°F. Recent data gathered by the Forest Products Lab for southern pine shows that a decrease in moisture content from 12 to 4 percent results in a 47 percent increase in compressive strength parallel to grain and a 48 percent increase in compression strength perpendicular to grain[12]. We believe this effect is generally species independent. If applied to the redwood data, the 150°F exposure alone (without change in MC) may decrease compressive strength by 30 percent.

On average, the cold values displayed a 46 percent increase in average crush strength compared to the ambient-hot values. Specimens with grain angles on the radial face showed larger increases in strength than those on the tangential face.

Table 9. Average Crush Strength for Target Grain Angle Groups for SG = 0.36, MC = 14%, and Rings = 12.6/in.

Target Angle Group	Combined Ambient-Hot Data Set Crush Strength MC=14% psi	Combined Ambient-Hot Data Set Crush Strength MC=5% psi	Cold Data Set Crush Strength psi	Ratio of Hot (MC=5%) to Ambient (MC=14%) psi	Ratio of Cold to Ambient (MC=14%) psi
0°	4620	5660	6350	1.23	1.37
5° R	4290	5220	6370	1.22	1.48
5° T	4410	5200	5970	1.18	1.35
10° R	3780	4090	6530	1.08	1.73
10° T	4190	5190	5880	1.24	1.40
30° R	2940	3690	4230 (SG = 0.33)	1.26	1.44
30° T	3320	3810	4980	1.15	1.50
90°	1010	1040	1420	1.03	1.41
				Avg: 1.17	Avg: 1.46

6.2 Material Stresses at Crush and the Limitations of Hankinson's Formula

It is obvious from our observations of crush failure of redwood at non-zero grain angles that shear failure plays a significant role in the failure process. Shear strength is not part of Hankinson's

formula (Eq. 2). Stresses must be transformed to the material coordinates to study the role of shear stress.

The nominal triaxial stress state imposed by the test device at the onset of crush failure can be mathematically transformed from the axis of the test device to the axis of the material orthotropy as depicted in two-dimensions in Fig. 9. This transformation is accomplished using Eq. 3, where the transformation matrix is shown in Eq. 4.

$$\sigma_{material} = [T]\sigma_{device}[T]^T \tag{3}$$

Three data subsets (series 300, 800, and 700) from the ambient data were studied to examine how the measured nominal device stresses transformed to the material axis system. Each set and specimens within each set had approximately the same specific gravity, ring count and moisture content.

The transformation matrix, T, was derived as part of this research and is shown in Eq. 4. This matrix is limited to ring angles of 0 or 90 degrees. A full transformation matrix without the ring angle restriction and proof of its validity was also developed. The unrestricted transformation matrix is described by Hermanson[13]. For measured surface angles of 0 degrees,

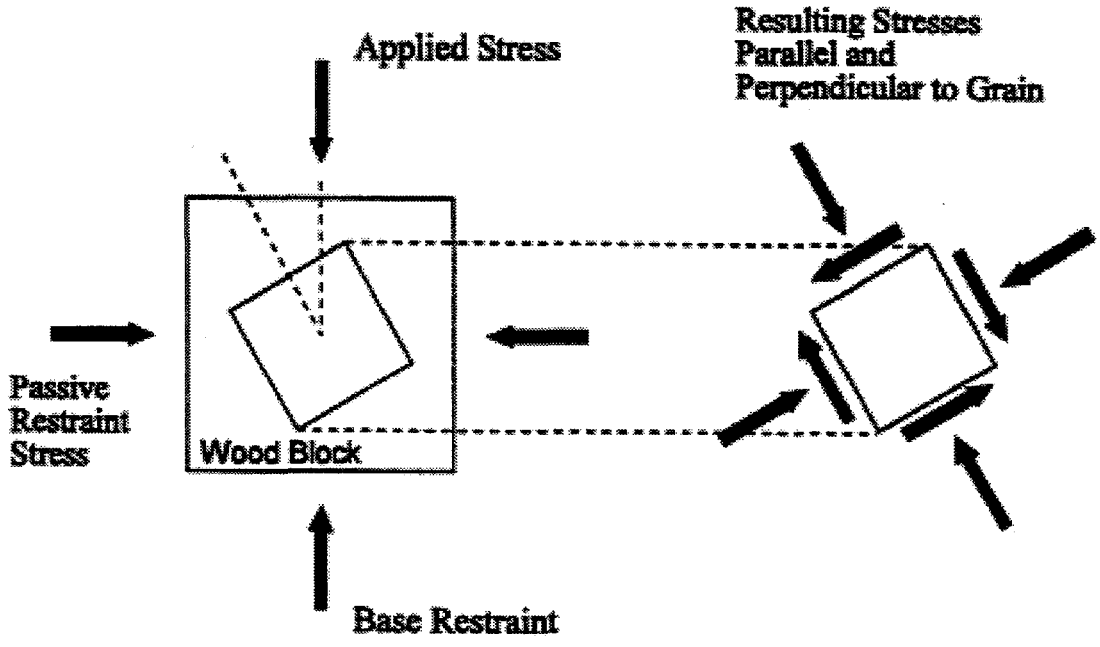

Figure 9. Transformation of Specimen Stress State to the Axes of the Material

the following key identifies the direction system:

1 Direction = Radial Direction (R)
2 Direction = Tangential Direction (T)
3 Direction = Longitudinal Direction (L).

$$[T] = \begin{bmatrix} \cos\alpha\cos\theta & \sin\alpha\cos\theta & -\sin\theta \\ -\sin\alpha\cos\beta + cos\sin\theta\sin\beta & \cos\alpha\cos\beta + \sin\alpha\sin\theta\sin\beta & \cos\theta\sin\beta \\ \sin\alpha\sin\beta + \cos\beta\cos\alpha\sin\theta & -\cos\alpha\sin\beta + \sin\alpha\sin\theta\cos\beta & \cos\theta\cos\beta \end{bmatrix}$$

where, β=arctan(cosθ tanγ)
γ=grain angle measured on the 2-3 face of the specimen, (see Fig. 3),
θ=grain angle measured on the 1-3 face of the specimen,
α= ring angle limited to values of 0 or 90° for Eq. 4.

For example, stresses before and after transformation for two specimens, C345 and C312, are shown in Table 10. Compressive stresses are positive. Based upon the measured Gamma and Theta, the specimen stresses in the axes of the test device are transformed to the normal and shear stresses in the material coordinate system (R, T, L axes). Target grain angles that were manufactured to occur on the radial face (such as with Specimen C345) resulted in predominant normal and shear stresses in the radial-longitudinal plane and specimens with grain angles on the tangential face (such as Specimen C312) produced predominant stresses in the tangential-longitudinal plane. The different grain angles result in different combinations of triaxial stress in the material coordinate system. Nominal stress states in the test device frame of reference were taken from the test data as load divided by original area and transformed according to Eq. 3 to yield a triaxial stress state in material coordinates.

Table 10. Original Device and Transformed Material Stresses for Specimens C345 and C312. Angles in Degrees and Stresses in psi.

Specimen	g	q	Untransformed Stresses in Test Device Coordinates			Transformed Stresses in Material Coordinates					
			s_1 psi	s_2 psi	s_3 appl. load psi	s_R psi	s_{R-T} psi	s_{R-L} psi	s_T psi	s_{T-L} psi	s_L psi
C345	3.2	28.5	301	154	1703	621	-29	-587	157	60	1381
C312	-27.4	2.5	254	305	3154	311	57	-110	866	-1182	2536

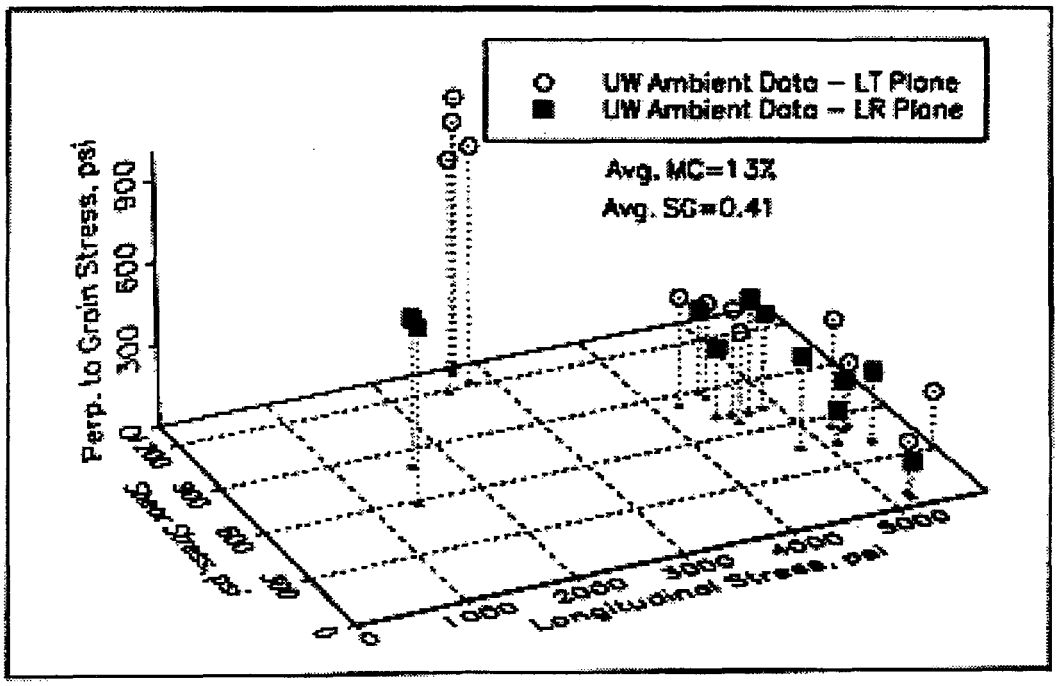

Figure 10. Stresses in the Material Coordinate Systemat Peak Crush Stress for Ambient Data Set

Figure 10 shows the resulting critical stress combinations that occur with otherwise similar specimens possessing grain angles from 0 to 30 degrees on the radial face or the tangential face. These points represent the crush initiation failure surface. Complete definition of the crush initiation failure surface will provide an alternative to Hankinson's formula. Figure 11 indicates that critical stress states are similar when grain angle is low resulting in high longitudinal stresses and low shear stresses. As grain angle increases and causes high shear stress, specimens with the grain angle on the tangential face are stronger than when the grain angle is on the radial face.

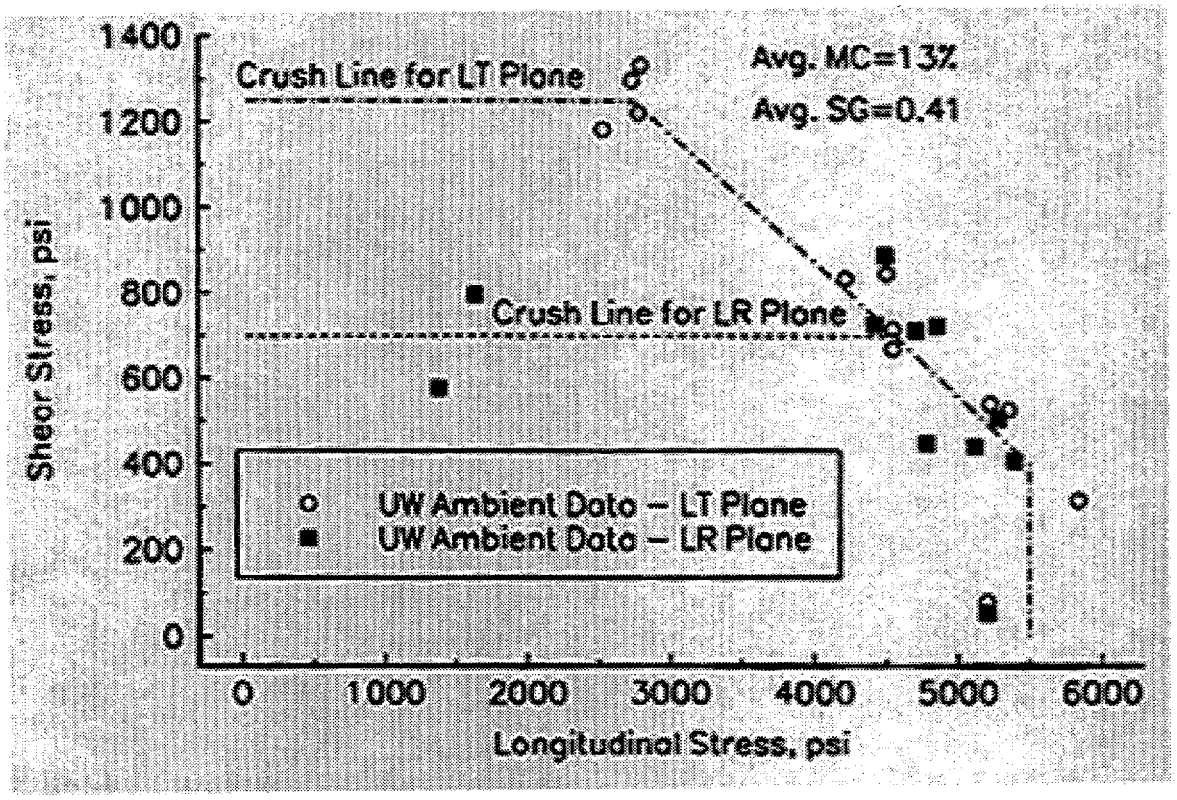

Figure. 11 Critical Combinations of Longitudinal and Shear Stresses for Ambient data Subset

Figure 11 shows the longitudinal-shear stress plane for the same data subset shown in Fig. 10. Figure 11 reveals a potentially simple crush failure theory:

1) longitudinal crush strength (5,500 psi) controls multiaxial crush for all specimens when shear stress is less than 400 psi,
2) from a shear stress of 400 psi to 700 psi in the LR plane and 400 psi to 1250 psi in the LT plane, an interaction of longitudinal stress and shear stress defines crush initiation,
3) a limiting shear stress of 700 psi in the LR plane and 1250 psi in the LT plane will define crush initiation.

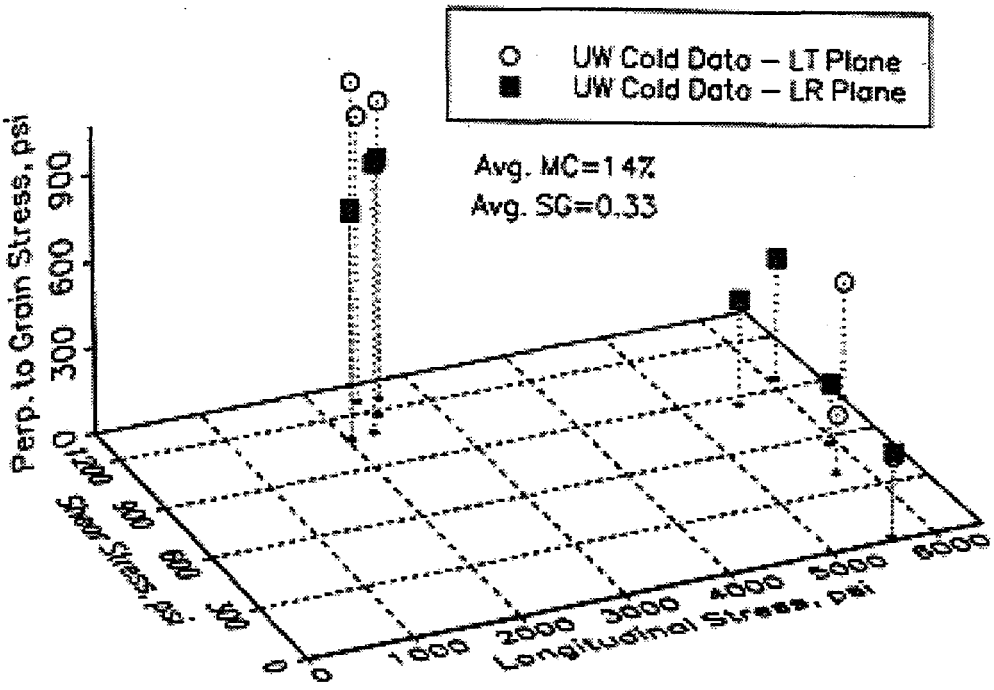

Figure 12. Stresses in the Material Coordinate System at Peak Crush Stress for Cold Data Subset

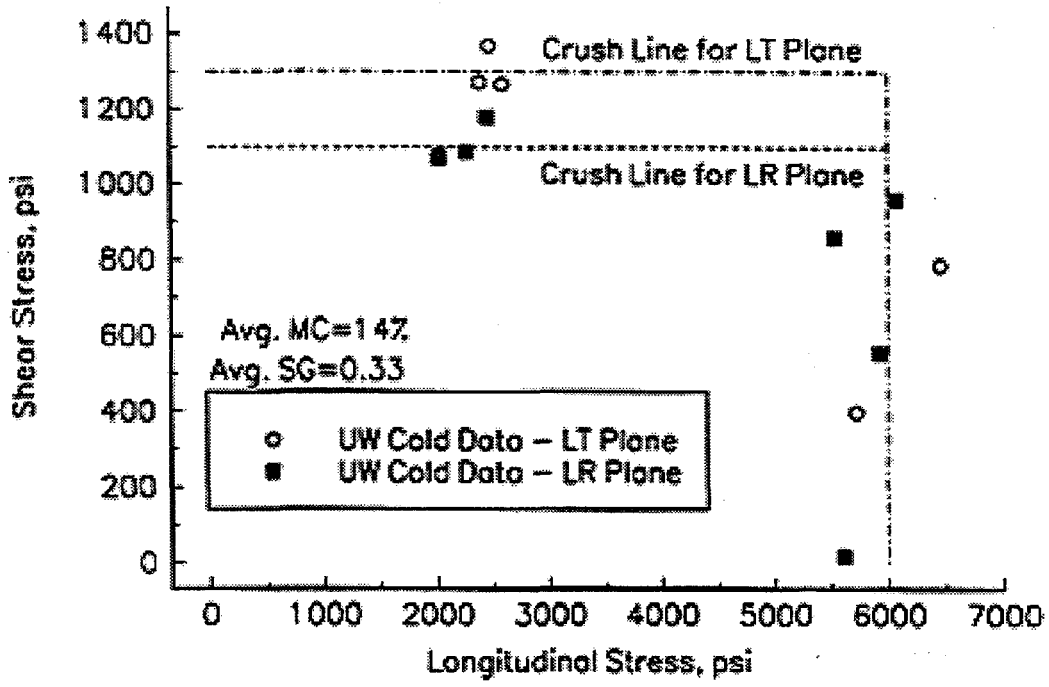

Figure 13. Critical Combinations of Longitudinal and Shear Stresses for Cold Conditions

1. limiting longitudinal stress of 6000 psi,
2. limiting shear stress in the LR plane of 1100 psi,
3. limiting shear stress in the LT plane of 1300 psi.

This potential theory shows that wood becomes more brittle material under cold conditions. The different strengths change individually as wood temperature changes from ambient to cold conditions.

6.3 Assessment of Leading Strength Failure Theories to Predict Redwood Crush at Angles to Grain

The previous discussion has indicated that Hankinson's Formula provides only a approximate prediction of crush stress at non-zero grain angles and that stress states with high shear stresses exist at crush for specimens with grain angles as low as 10 degrees. Given these stress states, is there a failure theory more sophisticated than Hankinson's Formula that can be used to predict crush failure and describe the crush failure surfaces?

Several different failure theories have been proposed for wood in the last 70 years, but all have encountered severe limitations in applicability to wood. Most recent attention has been directed to strength polynomial failure theories which are variations on that proposed by Tsai and Wu. Liu[14] has presented this theory as it applies to wood but without evidence that it predicts wood failure. As pointed out by Attaway[15], this theory has the advantage that established rules on transformation, invariance, and symmetry are applicable. Using the notation presented by Liu[14], this equation has the form:

$$F_i \sigma_i + F_{ij} \sigma_i \sigma_j = 1 \qquad (5)$$

where F_i and F_{ij} are functions of the uniaxial compressive and tensile strengths parallel and perpendicular to grain and shear strength parallel to grain. Liu[14] defined F_{12} such that Hankinson's formula is a special case of the strength polynomial theory. F_{12}, however, can take on a wide variation of values and the strength polynomial theory will still give roughly similar results to Hankinson's formula. This is important considering the inability of Hankinson's formula to precisely describe the data collected in this study.

For simplicity, if we initially consider only the predominant stresses in the LR plane and the LT plane as shown in Fig. 11, we can use the two-dimensional form of Eq. 5 to initially assess the viability of the strength tensor theory to predict crush strength. Shear strength in the RT plane is undocumented and is essential information to apply the full three dimensional form of the theory. Uniaxial strengths and resulting tensor polynomial values used are shown in Table 11.

Table 11. Redwood Strengths and Strength Polynomial Tensor

Strength Parameter	Strength Value, psi	Source	Strength Polynomial Parameter	Parameter Value
Tensile Str. Parallel to Grain, X, psi	10,622	USDA Wood Handbook[3]	F_1, $(psi)^{-1}$	-8.767×10^{-5}
Compressive Str. Parallel to Grain, X', psi	5,500	UW Redwood Data Subset	F_{11}, $(psi)^{-2}$	1.712×10^{-8}
Tensile Str. Perp. to Grain, Y, psi	240	USDA Wood Handbook[3]	F_2, $(psi)^{-1}$	3.167×10^{-3}
Compressive Str. Perp. to Grain, Y', psi	1,000	UW Redwood Data Subset	F_{22}, $(psi)^{-2}$	4.167×10^{-6}
Shear Str. Parallel to Grain LT Plane, S_{LT}, psi	1,250	UW Redwood Data Subset	$F_{12=LT}$, $(psi)^{-2}$	1.059×10^{-7}
Shear Str. Parallel to Grain LR Plane, S_{LR}, psi	700	UW Redwood Data Subset	$F_{12=LR}$, $(psi)^{-2}$	-5.945×10^{-7}
			$F_{66=LT}$, $(psi)^{-2}$	6.400×10^{-7}
			$F_{66=LR}$, $(psi)^{-2}$	2.041×10^{-7}

Table 12 shows the computed value for the three subsets of ambient crush data considered in the previous section. Two-dimensional failure index values are shown for F_{12} as required by Hankinson's formula and F_{12} equal to 0.0. If the strength polynomial failure theory offered a perfect prediction of crush failure for each specimen, the failure value in Table 12 would be 1.0. When the grain angle falls in the LR plane, F_{12} as required by Hankinson's formula causes the strength tensor theory to be a poor predictor of crush failure. When F_{12} is set equal to 0.0 failure predictions improve dramatically. When the grain angle falls in the LT plane, the strength polynomial theory under-predicts the failure index at low angles and shear stresses and over-predicts the failure index at high angles and shear stresses. This dichotomy emphasizes the important role played by shear stress in crush failure and the differences caused by similar grain angles in different planes. The strength polynomial failure theory is complex and requires strength data for each mode of possible failure. As indicated in the comparison here, it is sensitive to the interaction term, F_{12}. It is for these reasons it has never been successfully applied to wood. Further investigation of various F_{12} terms is needed before firm conclusions can be formed concerning the strength polynomial theory.

Table 12. Strength Polynomial Failure Index for Select Ambient Data at First Crush

Specimen	Target Grain Angle	Specific Gravity	2-D Strength Tensor Failure Index F_{12} (after Liu[14])	2-D Strength Tensor Failure Index, $F_{12} = 0.0$
C311	5 R	0.38	-0.90	0.77
C815	5 R	0.40	-0.14	1.02
C813	5 R	0.39	0.24	0.97
C843	5 R	0.41	-1.32	0.63
C316	10 R	0.38	-0.07	1.27
C816	10 R	0.39	0.11	1.77
C719	10 R	0.45	-1.15	1.24
C713	10 R	0.45	-0.74	1.30
C345	30 R	0.41	0.70	0.50
C718	30 R	0.44	-0.06	1.00
	Averages	0.41	-0.33	1.05
C321	5 T	0.38	0.89	0.62
C812	5 T	0.38	0.94	0.69
C746	5 T	0.41	0.96	0.51
C342	10 T	0.39	0.77	0.45
C817	10 T	0.41	0.94	0.60
C831	10 T	0.43	0.89	0.52
C715	10 T	0.44	0.86	0.48
C312	30 T	0.38	2.08	1.61
C344	30 T	0.39	3.44	2.55
C314	30 T	0.38	2.29	1.77
C711	30 T	0.43	2.67	2.13
	Averages	0.40	1.52	1.08

Another interaction failure formula frequently used with wood is that presented by Norris[16] and modified by others. This equation takes the form shown in Eq. 6.

$$I = \frac{\sigma_1^2}{S_1^2} I \frac{\sigma_1 \sigma_2}{S_1 S_2} + \frac{\sigma_2^2}{S_2^2} + \frac{\sigma_{12}^2}{S_{12}^2} \tag{6}$$

where,

1 and 2 refer to any two axes in the three-dimensional material coordinate system,

σ_i and σ_{ij} = normal and shear stresses in the direction of the ith axis,

S_i and S_{ij} = normal and shear strengths in the direction of the ith axis, and

I = an interaction constant taken as 1.0 in the original work by Norris.

The value of *I* originally presented by Norris was 0.0 and later was established as 1.0. Others have provided formulas for *I* that depend on material moduli or strength but the value is limited between 0 and 1. Physically, the *I* term suggests that biaxial compressive normal stresses will create an internal friction that will strengthen the material. This equation was evaluated for the ambient and cold data subsets shown in Figs. 11 and 13 using the corresponding limiting strengths indicated by that data. Table 13 shows the average Norris failure index value from Eq. 6 where a value of 1.00 indicates crush strength has been reached. The standard Norris equation where *I* equals 1.0 consistently underestimates the crush strength at both ambient and cold conditions. From our examination of the data it is clear that the Norris equation underestimates the strengthening effect of perpendicular-to-grain compressive stresses on the shear stress that can be sustained. As indicated in Table 13, this deficiency in the Norris Equation can be corrected by increasing the *I* value. Different values of *I* are needed to yield a successful Norris equation for the LT and LR planes, and for cold temperature conditions.

Table 13. Average Norris Failure Index Values for Ambient and Cold Data Subsets Stress States of Fig. 11 and 13.

I Value	1.0	1.0	1.40	2.75
Stress Plane	LT	LR	LT	LR
Failure Index - Ambient Data Subset - 22 points, Avg. MC= 13%, Avg. SG=0.41	1.14	1.40	0.99	1.00
I Value	1.0	1.0	2.0	2.1
Stress Plane	LT	LR	LT	LR
Failure Index - Cold Data Subset - 14 points, Avg. MC=14%, Avg. SG=0.33	1.24	.25	0.99	1.01

The Norris equation holds potential as an improved predictor of wood crush. Before adoption, however, it should be evaluated for a more comprehensive set of critical stress combinations and a rational justification for the *I* values should be established. Unpublished biaxial tension data for Douglas-fir collected by the senior author suggests that the Norris equation is not applicable to tension-dominated stress states. Furthermore, it is clear that crush strength behavior depends on the material plane of stress occurrence and on temperature. The evidence indicates that failure theory for wood depends on many factors and cannot be described by one simple theory and one set of parameters.

Why hasn't a successful crush failure theory been identified for wood? The data here combined with the work of others provides a clear answer. Redwood crush strength depends on grain

angle, specific gravity, moisture content, and temperature. As these parameters are changed, the controlling failure mechanism will change. Figures 7, 8, 11 and 13 show that different failure mechanisms control crush failure for angles on radial face versus the tangential face. Kretschmann and Green have shown that strengths change in Southern Pine for different moisture contents[12]. This effect is believed to be largely species independent. No single study has examined the interactions of all of these variables. One simple theory that explains failure for one limited set of conditions likely will not be accurate for another set of conditions resulting in apparent variability. A more comprehensive theory is needed for more sophisticated designs using wood.

7 Boundary Effects at Wood-Metal Interfaces

7.1 Test Device Friction

The failure analysis presented in Section 6.3 suggests that lateral confining stresses impose internal friction forces that increase the apparent shear strength of redwood material. Friction forces and other effects also occurred at the boundary of the redwood test specimen and steel test device. This situation has been acknowledged in previous sections by referring to *nominal* crush values. In addition to friction, material asperities on surfaces where wood sample meets steel test device are known to have influenced the test values. Analysis of boundary condition effects must be completed before the data collected in this test program can be fully utilized. In this study we attempted to minimize frictional forces along the confining side plates of the test device by applying a thin layer of paraffin to the steel side surfaces. Undoubtedly, frictional forces still occurred as some function of the lateral confining forces. The Wood Handbook[4] suggests that the coefficient of friction between wood and steel varies between 0.3 and 0.7 depending primarily on moisture content. Because this general range is so large, we conducted a small number of tests to provide a more precise estimate of the friction conditions in this test program.

Nine tests were conducted at ambient conditions. Lateral load was varied from 10 to 20 psi along the Longitudinal axis of wood specimen C221. Two tests were conducted with a thin coating of paraffin applied to the lateral restraint plates and seven tests were conducted with no paraffin. Six friction tests were conducted at -20° F with lateral normal pressures varying from 10 to 100 psi. Four of these tests were conducted on specimen C221 and two tests were conducted on specimen C849.

From these tests we have estimated that the applied force necessary to cause specimen/test device interface slippage under lateral compression is a constant applied force of 0.6 times the lateral confining force when there is no lubricant used. When paraffin is used to coat the interface surfaces (as in all of the crush tests in this study), we found the coefficient of friction dropped to 0.3. This value is thus used to estimate frictional boundary effects. This means that the crush strength from confined tests reported by other investigators as well as those nominal values reported in this report over-estimate the true crush strength of the material. Because the friction tests conducted were few in number and did not cover the full range of lateral confining forces, this section presents only an estimate of the frictional effects.

What is the effect of this estimated friction on the analysis previously presented? Table 14 shows the ratios between the reported nominal crush strengths and the estimated friction-free crush strengths. As specimens with increasing grain angles were crushed, higher lateral confining forces per pound of applied vertical force were observed. As a result, the ratios in Table 14 increase with increasing grain angle. Figure 14 shows the crushed data from Fig. 8 adjusted for the effect of friction. By comparing Figs.7 and 8 with Fig. 14, it can be seen that the ability of Hankinson's formula to predict crush for non-zero grain angles improves when estimated frictional effects are removed from the data. Data points at 30 degrees, however, are still under predicted.

Table 14. Ratios of Nominal Average Crush Strength to Estimated Friction-Free Average Crush Strength

Target Grain Angle Group	Nominal Avg. Crush Strength Over Friction-Free Avg. Crush Strength - Ambient Data	Nominal Avg. Crush Strength Over Friction-Free Avg. Crush Strength - Cold Data
0 degrees	1.08	1.12
5 degrees - R face	1.02	1.14
5 degrees - T face	1.08	1.14
10 degrees - R face	1.08	1.15
10 degrees - T face	1.09	1.16
30 degrees - R face	1.33	1.50
30 degrees - T face	1.10	1.32
90 degrees	1.38	1.39

Ambient stress states similar to those presented in Fig. 11 but with estimated friction effects removed are shown in Fig. 15. The general form of critical stress states remain largely unchanged and the stress values show only a small decrease. Fig. 16 shows cold data stress states, and again, the effect of estimated friction is a small decrease in critical stresses.

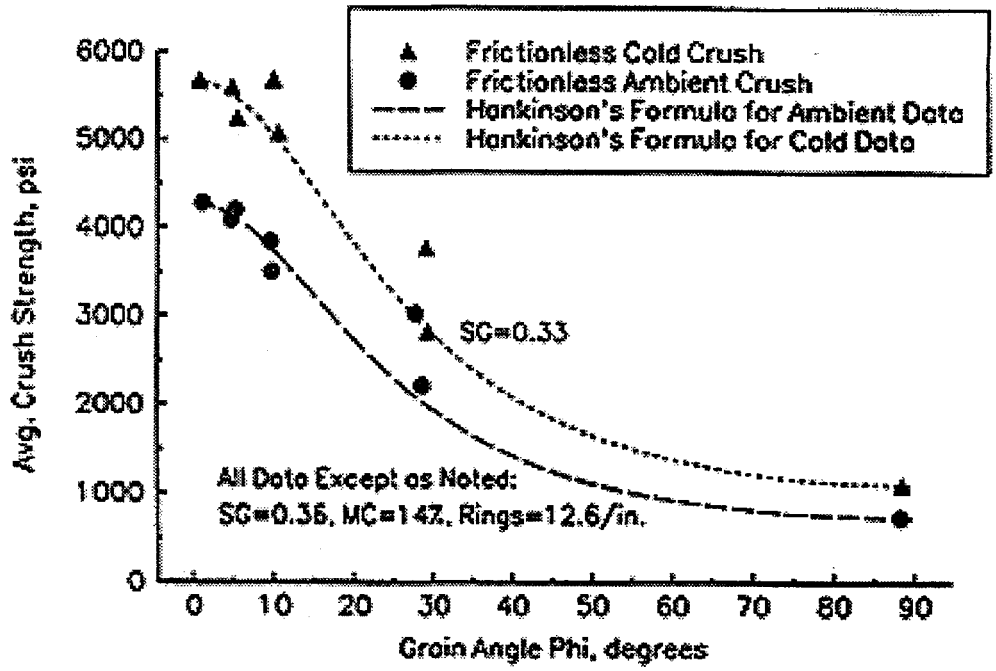

Figure 14. Average Crush Strengths for the Ambient and Cold Conditionsfor Friction and Shown with Hankinson's Formula

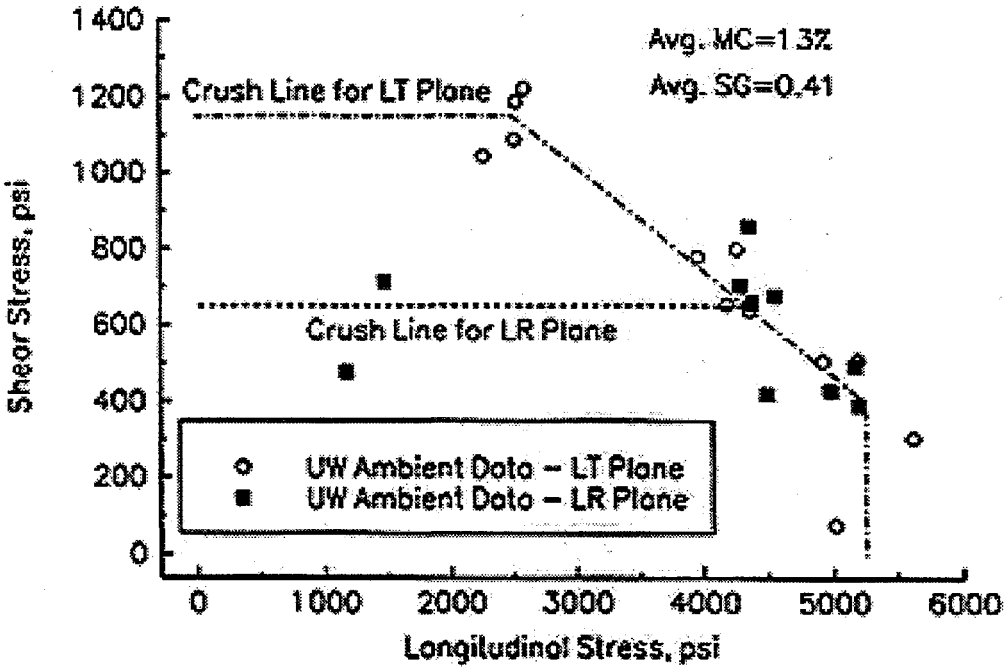

Figure 15. Critical Combinations of Longitudinal and Shear Stresses for Cold data Subset after Adjustment of the Applied Stress for the Estimated Friction. Compare to Figure 11

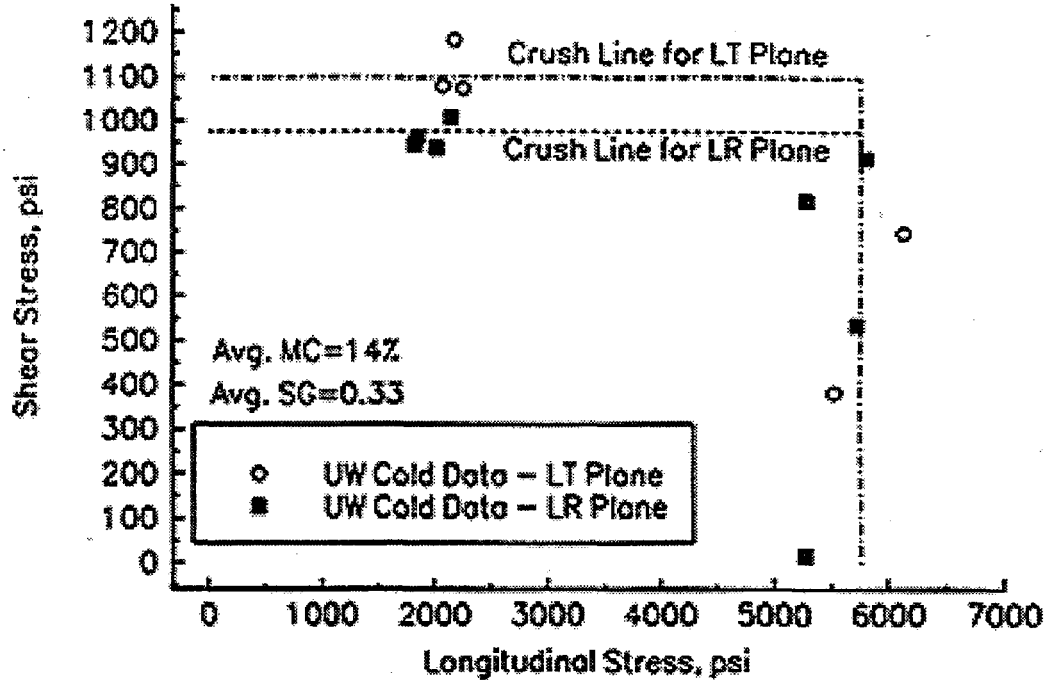

Figure 16. Critical Combinations of Longitudinal and Shear Stresses for Cold data Subset after Adjustment of the Applied Stress for the Estimated Friction. Compare to Figure 13

Lateral forces resulting in friction tend to increase with volumetric crush and larger grain angles produce larger lateral forces. For example, Figure 17 shows the stress-volumetric crush plot for specimen C533 possessing a 30 degree grain angle on the radial face. As indicated in Fig. 17, the amount of lateral force at crush is relatively small but increases significantly during the crush plateau. The amount of lateral force on each lateral axis is not equal because the grain angle renders the material axes unsymmetrical with respect to the device axes. As a result, friction forces are relatively small at crush strength for most grain angle and temperature conditions. True crush strengths are only slightly less than predicted when friction is ignored and the general trends are still valid. Friction forces continue to increase through the crush plateau, however, and cannot be readily ignored over the full crush zone.

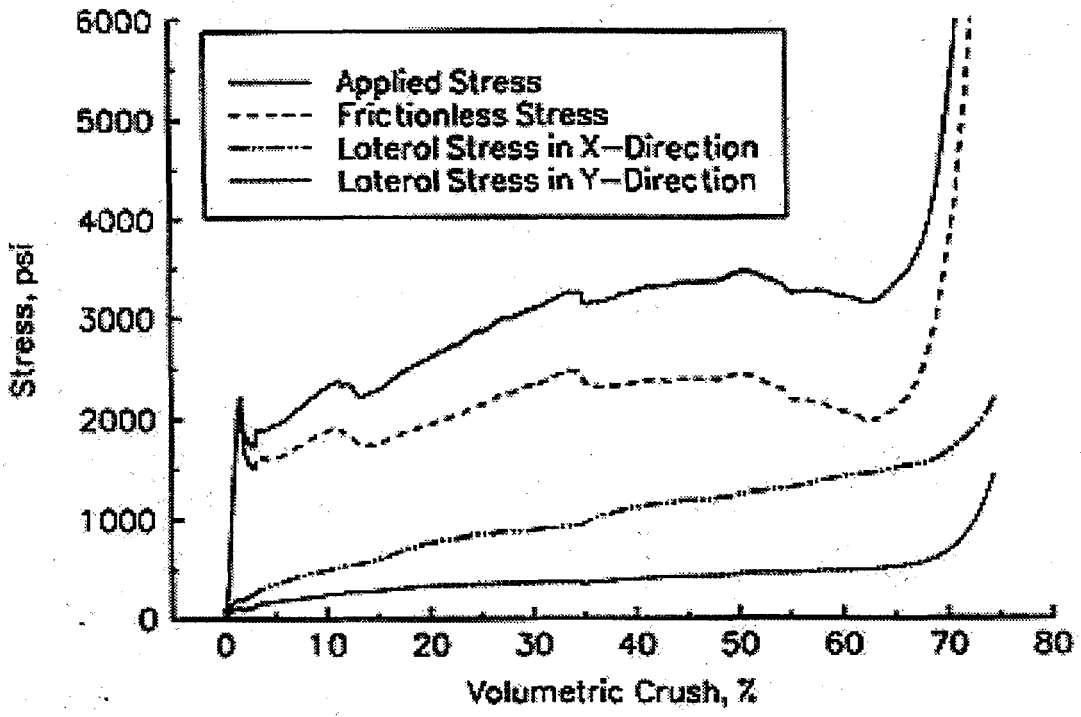

Figure 17. Stress-Volumetric Crush curves for Specimens C533 Showing Increasing Lateral Stresses and Increasing Frictional Effects

7.2 The Effect of Material Asperities and Frictional Restraint on Apparent Modulus of Elasticity

It has long been recognized that measurement of stress and strain to determine the modulus of elasticity of any material must occur in a central region of the specimen removed from the effects of boundary conditions. These boundary conditions consist of friction at the interfaces of the wood and steel as described in the previous section and the non-uniform distribution of surface stresses resulting from material asperities as described by Wolcott et al.[5] In the confined triaxial tests conducted in this research it was not possible to attach devices to the central portions of the specimen surfaces to measure strain. Instead, it was necessary to compute nominal strains from displacement measurements of steel platens on opposing sides of the specimen. These measurements included the boundary condition effects that are typically avoided.

To provide an estimate of the boundary condition effects, uniaxial tests at ambient temperatures were conducted on a small sample of redwood cubes. Tests were conducted in the longitudinal, radial, and tangential directions measuring displacement of the two ends of the 4 inch cube specimen and measuring displacements from a one-inch gage centrally located on an unloaded face. The modulus of elasticity was computed from the strains derived from the one-inch gage measurements and from displacements obtained from surface to surface of the specimen. The results of this analysis are shown in Table 15. Also shown in Table 15 are published values from Bodig and Goodman[17].

Table 15. Published and Measured Modulus of Elasticity Values

Redwood Direction	Published Modulus of Elasticty[16], psi	Avg. E-gage, psi	Avg. E-surface to surface, psi	Ratio E-gage/E-surface to surface
Longitudinal	1,523,000	1,237,000	615,000	2.1
Radial	131,900	82,200	43,600	1.9
Tangential	135,900	33,800	32,100	1.0

The gage values in Table 15 are within range of the published values for all directions except the tangential direction and are considered to be representative of the true modulus of elasticity. There are several possible reasons why the measured tangential direction moduli were unusually low, but the E-gage values are believed to be representative of tangential modulus of elasticity of the redwood material used in this study. The comparison between the realistic moduli established from gage measurements and the moduli computed from the surface to surface measurements shows a factor of difference of approximately 2 in the radial and longitudinal directions. This factor provides an indication of the important effect of material disparities in initial displacements occurring where wood meets steel.

8 Applied Stress-Volumetric Crush-Grain Angle Surfaces

Applied stress-volumetric crush-grain angle surfaces provide a means to quickly assess the energy absorbing characteristics of redwood. As with crush strength, the applied stress-volumetric crush curves are influenced by moisture content, specific gravity, temperature, and grain angle.

Figure 17 shows that lateral forces causing friction increase through the crush plateau and approaching material lockup. In the analysis presented here, the applied stress is adjusted for friction using the 0.3 coefficient of friction.

In the absence of a complete and workable crush theory that can explain the different complexities of redwood crush, a simple model is proposed consisting of three distinct phases:

1. **linear**, elastic response to initial crush,
2. **plastic** crush plateau, and
3. **densification** phase as the material reaches lockup.

When the wood fibers are subject to forces aligned with the longitudinal axis of the fiber (0° grain angle) , the data indicates that the transition between the different phases will tend to be abrupt. As the grain angle increases, the transition between phases will be more gradual, especially the transition to densification (compare Fig. 18 and 19). The empirical model accommodates these differences.

The three phases of crush response are modeled using two equations. The first equation (Eq.7) represents the linear response up to initial crush.

$$\sigma = (K)(volcrush) \tag{7}$$

where, σ = applied stress corrected for friction (psi),
K = slope of initial stress-volumetric crush response (psi),
volcrush = volumetric engineering strain.

The second equation (Eq. 8) models the crush plateau and densification phases.

$$\sigma = (M)(volcrush) + IS + K(volcrush)^P \tag{8}$$

where M = slope of crush plateau,
volcrush = volumetric engineering strain,
IS = stress at intercept of Eqs. 7 and 8,
P = densification power value.

Material densification occurs as the air-space voids are removed from the crushed material. This

dramatic increase in material stiffness is sometimes called material lockup. Wood cell wall material consists of cellulose and lignin, and because cellulose and lignin have similar densities, solid wood material (no voids), irregardless of species, has a common specific gravity of approximately 1.5[4,18]. As an alternative to the empiricism of Eq. 8, the volumetric crush strain for theoretically complete wood densification can be easily computed using the specific gravity of the wood under consideration and computing the strain needed for complete densification. For the average specific gravity of 0.37, complete densification would occur at a volumetric crush strain of 75%. The collected triaxial data showed a strong relationship between specimen specific gravity and the crush strain associated with the onset of material densification[19]. For low grain angle loading conditions, densification began abruptly at 60% volumetric crush strain. For high grain angle loading conditions, material densification began gradually at 40% volumetric crush strain but continued to increase. High grain angle situations approach the same slope of densification as low grain angle situations, but at slightly higher levels of volumetric crush. It is likely that all grain angle situations converge toward the volumetric crush associated with complete densification. For practical purposes, one may use 80% of the volumetric crush strain at theoretically complete densification for describing material lockup. As expected, the trends associated with material densification are independent of the temperatures considered because these temperatures and moisture contents did not impact the void ratio of the material.

The initial slope, K, of Eqs. 7 and 8 is normally expected to be the modulus of elasticity in a uniaxial test. These tests are not uniaxial and are influenced by boundary conditions, but K is likely some function of the elastic material constants. It was found that K possessed the strongest correlation with the friction-free average crush strength. Recall that crush strength and the crush strength relationships presented in Sections 5 and 6 consisted of the average nominal stress from 10 to 40 percent volumetric crush. These values can be corrected for the estimated friction using Table 14. Once friction-free crush strength values are established they can be used as the basis for computing crush curves. For ambient conditions, K can be predicted from the regression equation shown in Eq. 9 and similarly from Eq. 10 for cold conditions.

$$K_{amb} = 179.5(\sigma_{crush})48900 \tag{9}$$

$$K_{cold} = 132.4(\sigma_{crush}) + 2718 \tag{10}$$

where, K_{amb}= initial slope for ambient crush curves,
K_{cold}= initial slope for cold crush curves,
σ_{crush}= crush strength, avg. stress (10 to 40 percent vol. crush) adjusted for friction.

Values for parameters M and P in Eq. 8 were established as average values for each target grain angle group. These values are shown in Table 16.

Table 16. Crush Curve Values for Parameters M and P in Eq. 8.

Target Grain Angle Group	Ambient Conditions		Cold Conditions	
	M (Plateau Slope)	P (Densification Power)	M (Plateau Slope)	P (Densification Power)
0°	450	15	250	14
5° - R	570	13	220	14
5° - T	20	13	-290	14
10° - R	50	12	260	13
10° - T	90	12	-1860	12
30° - R	570	10	1780	14
30° - T	510	12	70	14
90°	640	9	930	10

For illustration, Figure 18 and 19 show the fit of the two-equation model for the specific cases of test C138 and test C645. Considering its simplicity, the model is a good predictor of crush performance and can be used to simulate the data collected in this study.

A crush curve can be predicted using the following procedure:

1. Establish the average crush strength for the desired SG, MC, RINGS, PHI and temperature using the relationships presented in Section 5.
2. Adjust the average crush strength for the effects of friction using Table 12.
3. Compute the corresponding initial slope, K using Eq. 9 or 10 using the avg. crush stress from step 2..
4. Solve for the intercept stress, IS, in Eq. 8 by setting σ=avg. crush stress from step 2.
5. Plot each Eq. 7 and 8 with Eq. 7 valid from $\sigma = 0$ to IS and Eq. 8 for $\sigma \geq$IS.

Following this procedure, surfaces can be created showing the how the crush curve changes with grain angle. Figure 20 shows the crush surface for ambient conditions and when the grain angle, Phi, occurs on the radial face of the specimen and Fig. 21 corresponds to specimens with the grain angle on the tangential face.

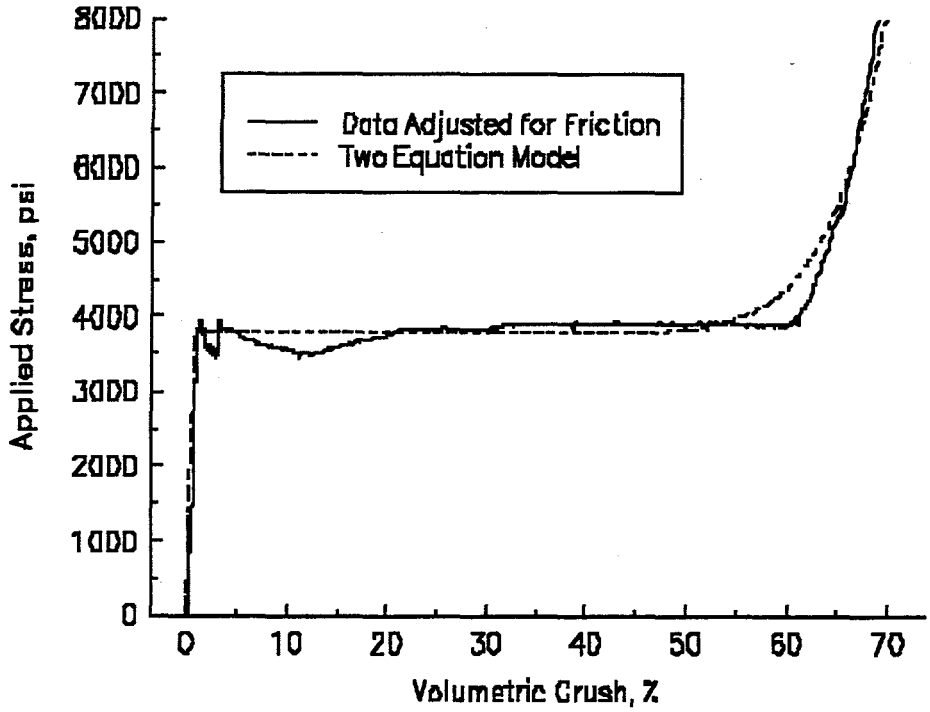

Figure 18. Two Equation Model Fitted to data from test C138 -5° T Ambient Test Conditions

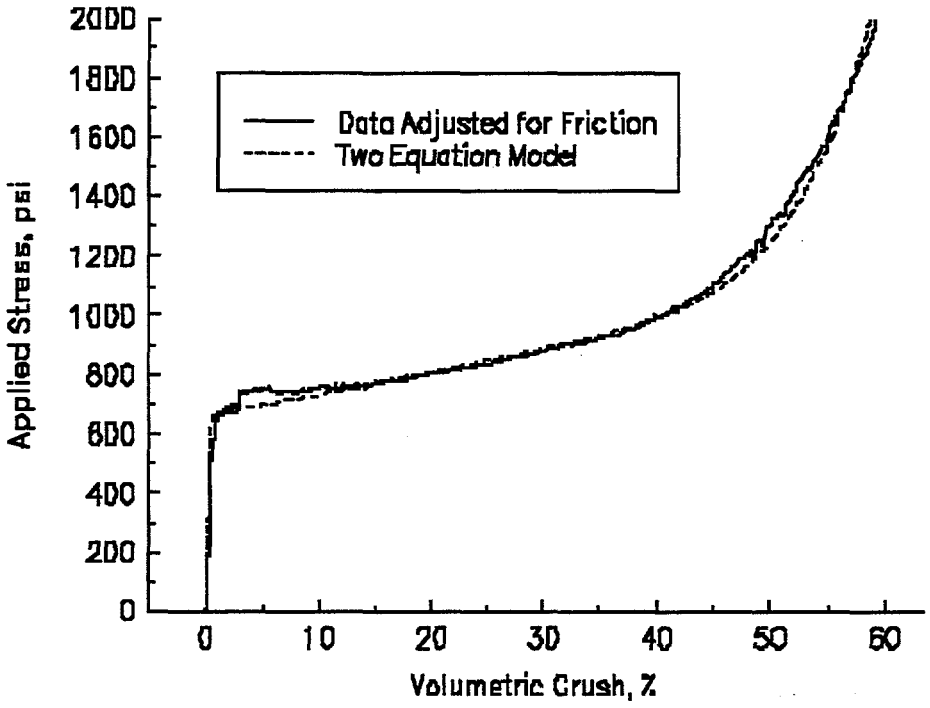

Figure 19. Two Equation Model Fitted to Data from test C645 -90° T Ambient Test Conditions

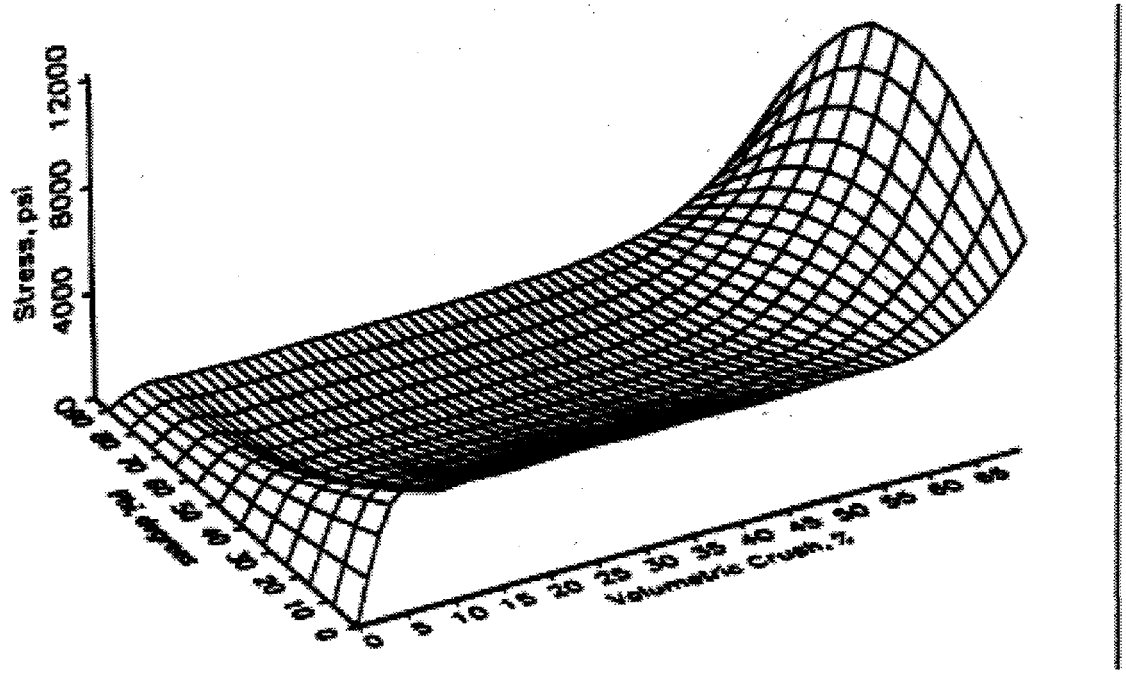

Figure 20. Crush Surface for Redwood at Ambient Temperature, SG=0.36, MC=14%,%, Rings=12.6/in.. and Grain Angle on the R Face.

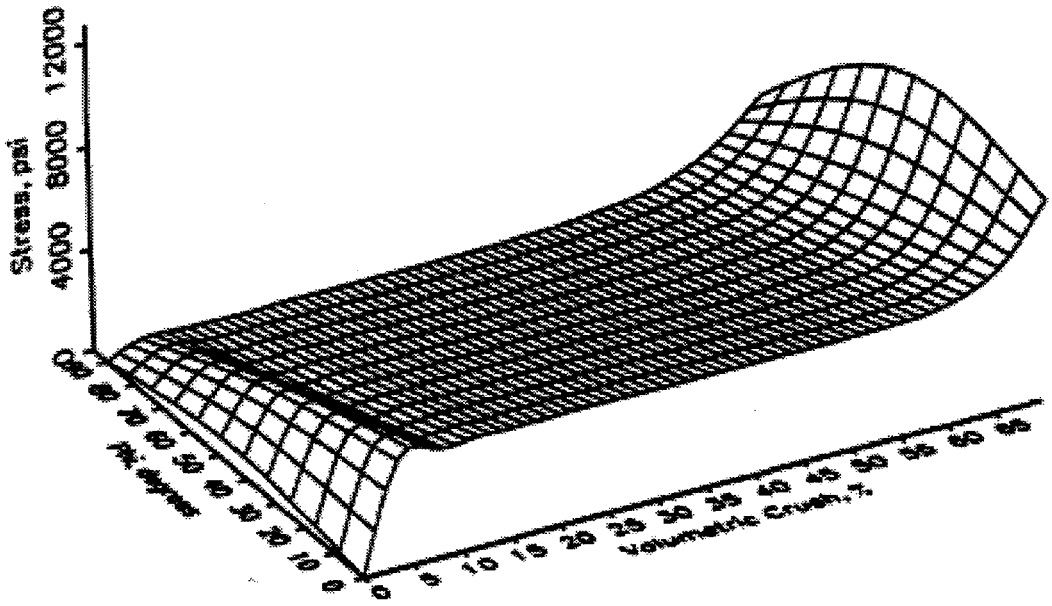

Figure 21. Crush Surface for Redwood at -20•F, SG=0.36,, MC=14%, Rings=12.6/in. and Grain Angle on the T Face.

9 Toward a General Stress-Strain Model for Redwood

Structural design has traditionally relied upon knowledge or computations of engineering stress

and strain. Impact limiter design or any application involving wood crush also needs to be based on material stresses and strains to allow general application of the design procedure. Full development of such a theory was beyond the scope of this research. Never-the-less, several noteworthy preliminary findings have been achieved from the analysis of the data collected.

The development of a general stress-strain model must address the three ranges of behavior previously identified:

1. **linear**, elastic response to initial crush,
2. **plastic** crush plateau, and
3. **densification** phase as the material reaches lockup.

Wood has long been modeled as a rectilinear, orthotropic, elastic material. Acceptance of this assumption has allowed the use of Hooke's Law to model stress-strain response:

$$\begin{pmatrix} \varepsilon_R \\ \varepsilon_T \\ \varepsilon_L \\ \gamma_{TR} \\ \gamma_{LR} \\ \gamma_{LT} \end{pmatrix} = \begin{bmatrix} \frac{1}{E_R} & \frac{-\nu_{TR}}{E_T} & \frac{-\nu_{LR}}{E_L} & 0 & 0 & 0 \\ \frac{-\nu_{RT}}{E_R} & \frac{1}{E_T} & \frac{-\nu_{LT}}{E_L} & 0 & 0 & 0 \\ \frac{-\nu_{RL}}{E_R} & \frac{-\nu_{TL}}{E_T} & \frac{1}{E_L} & 0 & 0 & 0 \\ 0 & 0 & 0 & \frac{1}{G_{TR}} & 0 & 0 \\ 0 & 0 & 0 & 0 & \frac{1}{G_{LR}} & 0 \\ 0 & 0 & 0 & 0 & 0 & \frac{1}{G_{LT}} \end{bmatrix} \begin{pmatrix} \sigma_R \\ \sigma_T \\ \sigma_L \\ \tau_{TR} \\ \tau_{LR} \\ \tau_{LT} \end{pmatrix}$$

where,

$\__i$= normal strain in the ith direction,
γ_{ij}= shear strains in the ij plane,
ν_{ij}= Poisson's ratio in the ij plane,
E_i= modulus of elasticity in the ith direction,
G_{ij}= shear modulus in the ij plane,
R = radial material axis,
T = tangential material axis,
L = longitudinal material axis.

Elastic properties as needed in Hooke's Law have been gathered over the past 75 years for many commercial species to provide an engineering database for wood design. For redwood the most complete set of elastic properties is presented in Table 17. These properties were gathered in a study by Bodig and Goodman from a single redwood log[17].

Table 17. Elastic properties for redwood after Bodig and Goodman[17]

Source	Moist. Content, %	Density (g/cm^3)	Elastic Modulus, E_L, psi	Elastic Modulus, E_R, psi	Elastic Modulus, E_T, psi	
Simpson Timber Co., Korbel, Calif.	10.9	0.388	1,523,000	131,900	135,900	
Shear Modulus, G_{LR}, psi	Shear Modulus, G_{LT}, psi	Shear Modulus, G_{RT}, psi	Poisson's Ratio, ν_{LR}	Poisson's Ratio, ν_{LT}	Poisson's Ratio, ν_{RT}	Poisson's Ratio, ν_{TR}
100,300	117,900	11,710	0.360	0.346	0.373	0.400

Hooke's Law is limited to elastic response so it has little value for computations involving wood crush. Yet, because of its long history and associated elastic property database, it provides an accepted starting point in developing a more general stress-strain law. The concepts of elastic and shear moduli and Poissons ratio are fundamental to engineering materials and thus these concepts are retained in the framework for a new constitutive model.

In preliminary developments toward a general stress-strain law, a general form similar to Hooke's Law was adopted as shown in Eq. 12 where A through L represent stiffness functions to describe the nonlinearity of properties through the crush range. By taking the inverse of the matrix in Eq. 12 within the linear range of material response a form comparable to Hooke's Law in Eq. 11 is obtained.

$$\begin{pmatrix} \sigma_R \\ \sigma_T \\ \sigma_L \\ \tau_{TR} \\ \tau_{LR} \\ \tau_{LT} \end{pmatrix} = \begin{bmatrix} A & B & C & 0 & 0 & 0 \\ D & E & F & 0 & 0 & 0 \\ G & H & I & 0 & 0 & 0 \\ 0 & 0 & 0 & J & 0 & 0 \\ 0 & 0 & 0 & 0 & K & 0 \\ 0 & 0 & 0 & 0 & 0 & L \end{bmatrix} \begin{pmatrix} \varepsilon_R \\ \varepsilon_T \\ \varepsilon_L \\ \gamma_{TR} \\ \gamma_{LR} \\ \gamma_{LT} \end{pmatrix} \quad (12)$$

Assuming the use of nominal stresses and strains computed from the test data, Eq. 12 presents a series of 6 equations with 12 unknowns, resulting in an under-determined system of equations. The unknowns are the stiffness functions A through L. As the number of unknowns exceed the number of equations, a unique solution cannot be established. Assuming a symmetric matrix consistent with Hooke's Law such that B=D, C=G, and F =H in Eq. 12 and neglecting shear behavior, the system of equations is modified to 3 equations with 6 unknowns involving A, B, C, E, F, and J. The system of equations remains undetermined and an unique solution cannot be established from the test data.

Singular value decomposition provides a minimum solution with an orthonormal basis range of the null space spanning all feasible solutions for an under-determined system of equations. This technique provides a means to evaluate possible valid solutions, even though a unique solution cannot be found. Hermanson presents the details of the application of this well-known mathematical technique to the redwood tests conducted in this study[13]. A most likely solution derived from a subset of data tested under ambient temperatures is presented in Table 18.

Table 18 reveals a close comparison between elastic properties established from triaxial tests and those from uniaxial tests. The one exception to this observation concerns the Poisson's ratio in the LR plane and material interactions in the longitudinal and radial planes warrant further examination. Three conclusions can be drawn from Table 18. First, Hooke's Law is a reasonable model for the small-strain elastic response of redwood. Secondly, nominal stresses provide a sufficient approximation to the true stress state in the triaxial tests to allow their use for data analysis. Finally, this reasonably close comparison of elastic properties from triaxial and uniaxial tests provides convincing evidence that proposed models for triaxial redwood stress-strain response can be evaluated using the singular value decomposition method developed by Hermanson. This method can be extended to examine possible triaxial models for stress-strain response in the crush plateau and densification ranges[13].

Table 18. Comparison of Elastic Properties Established from Triaxial and Uniaxial Test Data

	Value from Singular Value Decomposition Analysis of Triaxial	

Elastic Property	Test Data	Values from Uniaxial Tests
Modulus of Elasticity - Longitudinal Direction	732,200 psi	615,000 psi (from Table 15)
Modulus of Elasticity - Radial Direction	40,800 psi	43,600 psi (from Table 15)
Modulus of Elasticity - Tangential Direction	34,800 psi	32,100 psi (from Table 15)
Poisson's ratio - RT	0.39	0.37 (published value from Table 17)
Poisson's ratio - LR	0.01	0.36 (published value from Table 17)
Poisson's ratio - LT	0.26	0.35 (published value from Table 17)

10 Strain Rate Effects on Wood Properties - A Review of Existing Knowledge

The developments presented in this report are based on quasi-static applications of load at a strain rate in the range of 0.35 percent to 6.6 percent per minute. These rates are substantially below those likely encountered in impact limiters and thus this section reviews existing knowledge on the effect of strain rate on wood properties.

Most engineering applications of wood do not consider functional utilization of the material past the presumed linear, elastic range and as a result the literature addressing strain rate effects is extremely limited. Much of the literature examines load rate effects in the context of efficient proof loading for lumber quality control[20,21,22]. These studies examined tension and bending and the load rates do not come close to those associated with impact limiters. The motivation for this research was to quantify the effect of more rapid loading rates to allow more efficient proof-loading operations in lumber mills. Other studies including that by Gerhards[23] have examined loading rates in the context of long duration loads and creep - the opposite of impact loading.

The earliest comprehensive study of the properties of redwood was presented by Luxford and Markwardt[9]. Their study consisted of a specific-gravity survey and mechanical tests on both virgin and second growth small clear specimens of redwood. The source of material was from the commercial growing area of redwood beginning just north of San Francisco, Calif. and extending north along the coast to the California state border. The most relevant conclusion from the specific-gravity survey was that virgin redwood possessed the highest specific gravity followed by second growth trees which were closely grown, followed by second growth tress which were openly grown. In all cases the specific gravity ranged from .30 to .45 both within individual logs and between different logs, except for wood very near the bark layer.

Luxford and Markwardt also compared the shock resistance in bending of different species of wood. The data was developed by dropping a 50 pound hammer on a small, clear beam. Although this does not directly relate to impact absorption, such a shock resistance may be indirectly related. The shock bending ranking is listed in Table 19 with redwood providing the basis value of 100 percent. Also provided in the last column are the relative compressive strengths parallel to grain.

Only one reference was identified that specifically examined the effect of rapid loading on the compressive response of wood prior to the 1970's[24]. Liska published a study in 1950 where old-growth (250 to 400 years old) Sitka spruce and Douglas-fir 1 by 1 by 4 inch specimens were subject to various rates of compression loading. His findings are summarized in Table 20. These effects were considered small in consideration of other variability's related to wood properties.

Table 19. Relative Shock Resistance of Wood Species. Compiled from data of Luxford and Markwardt[9]

Commercial Species Name	No. of Trees Tested	Relative Bending Shock Resistance in Percent	Relative Compressive Strength Parallel to Grain in Percent
Cedar, Port Oxford	14	175	84
Pine, shortleaf	12	171	101
Pine, longleaf	34	158	119
Pine, loblolly	10	143	101
Douglas-fir, coast	34	125	104
Cedar, eastern red	5	122	87
Cypress, southern	26	117	89
Spruce, Sitka	25	117	73
Hemlock, western	18	112	82
Fir, lowland white	10	111	80
Fir, silver	6	108	74
Fir, noble	9	105	74
Douglas-fir, Rocky Mtn.	10	103	81
Redwood	**16**	**100**	**100**
Pine, western white	14	100	73
Fir, white	20	92	71
Pine, ponderosa	31	89	67
Pine, sugar	9	85	66
Pine, northern white	18	85	65
Cedar, western red	15	80	72
Cedar, northern white	5	72	60

Table 20. Effect of Strain Rate on Compressive Response of Softwoods Parallel to Grain. Compiled from data by Liska[24]

Nominal Strain Rate, Strain per minute	Relative Sitka Spruce Max. Crush Strength	Relative Douglas-fir Max. Crush Strength	Relative Sitka Spruce Mod. of Elasticity	Relative Douglas-fir Mod. of Elasticity
0.3%	100%	100%	100%	100%
2.2%	107%	108%	103%	105%
9.9%	114%	113%	106%	107%
19.3%	117%	114%	107%	105%
50.0%	120%	119%	107%	107%
70.0%	120%	121%	106%	107%

Liska concluded that as loading rate is increased by 100 percent, a 2.5 percent increase in maximum crushing strength will occur. Increases in modulus of elasticity were slight. The strain at ultimate load in compression parallel to grain is approximately constant for all loading rates in softwoods.

Hill and Joseph[6] published results of a study examining the energy-absorbing characteristics of materials. The object was to provide an initial screening of energy-absorbing potential of materials including wood, various wood-fiber composites, several man-made foams and various fiber-additive concrete's. Specimens 5 inches in diameter by 6 to 8 inches long were tested in compression in a partially-confining steel tube. Both static and dynamic tests were conducted with the dynamic tests consisting of gas-charged propulsion of the specimen assembly into a 5000 lb. steel mass. Perhaps the most important parameter measured in these tests was specific energy. Specific energy (units of ft.-lb/lb) was computed for each specimen as the area under the force-deflection curve divided by the material weight. Three important conclusions were provided:

1. The specific energy of the confined materials tested were generally unaffected by strain rate (up to 300 ft./sec.).
2. The specific energy determined statistically by compression to large strains (greater than 50%) may be used as a design parameter for configuring impact limiters.
3. Wood materials compressed along the grain are the most effective materials for absorbing kinetic energy.

For the redwood loaded parallel to grain, the Hill-Joseph data shows dynamic specific energies to be 15 to 16 percent higher than the corresponding static value, although the statistical significance

of this increase is not clear. Perpendicular to grain the dynamic specific energies ranged from 2 to many multiples of the static values.

Reid et al.[25] conducted both static crush and dynamic penetration tests on yellow pine and American oak. American oak is not one of the major species of the red or white oak group[26] and thus it is not clear exactly what type of oak was tested. The comparison of test types showed that in the dynamic test initial stresses jump to 3 or 4 times the static crush strength before stresses level off to values slightly higher than the static crush level.

Two displacement rates were used in our testing of redwood cubical specimens. A rate of 0.014 inches per minute was used for the first ten minutes of each test and then a second rate of 0.263 inches per minute was used for the remainder of the test corresponding to strain rates of 0.35 percent and 6.6 percent strain per minute. The switch over from one rate to the other occurred in within one or two seconds and during this time the load head of the testing machine accelerated to the new speed. Close examination of Figs. 17, 18, and 19 reveal a jump in the applied stress-volumetric crush curves at approximately 3 percent volumetric crush. This acceleration of the load head of the test machine resulted in a short-term 10 percent increase in the crush strength. It appeared that the stress-volumetric crush path was disturbed only within a short amount of time associated with the acceleration. We propose that changes in acceleration and deceleration may have a greater influence on crush behavior than changes in constant rates of loading. The observations of Reid et al. related to sharp increases in initial stresses may support this proposal. No literature directly addressing the compressive behavior of wood subject to varying degrees of accelerated or decelerated loadings were found.

11 Summary of Accomplishments and Conclusions

This study has consisted of a test program, data analysis, and preliminary model development to establish a plasticity theory for wood and to assess the ability of failure models to predict wood crush strength. This data provides the most complete set of large-strain data for redwood known to be in existence. As part of the study the following major accomplishments were realized:

1) A triaxial load-deformation device based on passive restraint was designed and used to gather the first triaxial load-deformation data for wood.

2) Over 100 confined crush tests of redwood were conducted with grain angles ranging from 0 to 90 degrees. Three temperatures conditions were investigated: -20° F (Cold), Ambient (approx. 70° F), and +150° F (Hot).

3) A preliminary method for analyzing nominal stress-strain data from the triaxial tests was developed to allow evaluation of different stress-strain models.

4) The state-of-the-art in wood constitutive modeling, wood crush behavior, and strain rate effects were established from the literature and compared with the data collected.

5) An empirical method is presented to compute the stress volumetric crush-strain curve for different grain angles and temperature conditions.

Analysis of the data gathered in this test program has led to eight major conclusions as follows:

1) Specific gravity, ring count, moisture content, grain angle and temperature are all important parameters that control the crush behavior of wood. Specific gravity and ring count are related but some reduction in variability is achieved by using both parameters in crush strength predictions.

2) Nominal cold crush strength was on average of 46 percent greater over the range of grain angles than ambient crush strength for similar specific gravity and moisture contents.

3) Nominal hot crush strength was on average 17 percent greater than nominal ambient crush at the same specific gravity. This difference was attributed primarily a difference in average moisture content (5% for hot conditions and 14% for ambient conditions). The effect of decrease in moisture content more than offset the effect of an increase in temperature.

4) When the grain angle occurs on the tangential face crush behavior is significantly different than when the grain angle occurs on the radial face. This is likely the result of differences in shear strength and shear moduli between the two planes.

5) Hankinson's formula is an interpolation scheme rather than a realistic failure formula and provides only marginal predictions of crush strength at angles to the grain.

6) It is more rational to base predictions of crush strength on triaxial material stresses in redwood rather than applied stresses at angles to grain. The Norris equation holds potential as a crush strength predictor. Interactions between stresses causing crush failure change with temperature and plane of the grain angle. The Norris equation can be adjusted with an interaction constant that is 40 to 175 percent greater than that suggested in the literature to accommodate these differences. Because the normal stress interactions are much larger than suggested by existing theory, a greater understanding of the justification of the interaction is needed. The strength tensor polynomial theory (Tsia-Wu) did not adequately predict failure for 30° grain angle specimens, but more study and material property data are needed to form conclusions concerning the potential of this theory.

7) Friction forces in these confined tests increased nominal crush strengths by 2 to 38 percent for ambient conditions and 12 to 50 percent for cold conditions. This emphasizes the importance of accounting for boundary conditions including friction and material asperities when interpreting data from confined crush tests

8) Large increases in strain-rate (0.3 to 70 percent strain/minute) cause at most a 20 percent increase in crush strength parallel to grain. Strain-rate effects may be greater for perpendicular to grain situations. The test data gathered as part of this research suggests that changes in acceleration/deceleration may have a larger influence on redwood crush properties than changes in constant strain rate.

12 Literature Cited

1. Cramer, S. M. and Hermanson, J. C. (1991) Review of Literature Related to Constitutive Behavior and Crush Failure of Redwood. Sandia No. 66-1924, Project Report. Univ. of Wisconsin-Madison, Madison, Wisconsin. 18 pas. 1991.

2. Cramer, S. M. and Hermanson, J. Test Design Plans and Procedures for Wood Crush Modeling, SNL Contract 66-1924, University of Wisconsin-Madison, Madison, Wisconsin.

3. Cramer, S. M. and Hermanson, J. (1992) Test Data Report on Wood Crush Modeling, SNL Contract 66-1924, University of Wisconsin-Madison, Madison, Wisconsin.

4. US Dept. of Agriculture, Forest Products Laboratory (1987) *Wood Handbook Wood as an Engineering Material,* USDA Forest Service, Agriculture Handbook 72, Washington, DC, 466 pas.

5. Wolcott, M. P., Kasal, B., Kamke, F. and Dillard, D. (1989) Testing Small Wood Specimens in Transverse Compression, *Wood and Fiber Science,* 21(3), pas. 320-329.

6. Hill, T. K. and Joseph, W. W. (1974) Energy-Absorbing Characteristics of Materials, SLA74-0159, Sandia National Laboratories.

7. Joseph, W. W. and Hill, T. K. (1976) Energy-Absorbing Characteristics of California Redwood Subjected To High Strain, SAND-76-0087, Sandia National Laboratories.

8. Von Riesemann, W. A. and Guess, T. R. (1978) The Effects of Temperature on the EnergyAbsorbing Characteristics of Redwood, SAND77-1589, Sandia National Laboratories.

9. Luxford, R. F. and Markwardt, L. J. (1932) The Strength and Related Properties of Redwood. Technical Bulletin No. 305, US Dept. of Agriculture, 48 pas.

10. Gerhards, C.C. (1982) Effect of Moisture Content and Temperature on the Mechanical Properties of Wood: An Analysis of Immediate Effects, *Wood and Fiber,* Vol. 14, No. 1, pp. 436.

11. Engineering Division, Air Service, McCook Field, Dayton Ohio (1921) Investigation of Crushing Strength of Spruce at Varying Angles of Grain, Air Service Information Circular, Vol. III, No. 259, Chief of Air Service, Washington, DC

12. Kretschmann, D. E. and Green, D. W. (1994) Moisture Content and the Properties of Clear Southern Pine. USDA Forest Service, Forest Products Lab. Research Paper FPL-RP-531, 28 pas.

13. Hermanson, J. C. (1990) The Triaxial Behavior of Redwood using a New Confined Compression Device. Ph.D. Dissertation in-progress, Department of Civil and Environmental Engineering, University of Wisconsin-Madison, Madison, Wisconsin.

14. Liu, J. Y. (1984) Evaluation of the Tensor Polynomial Strength Theory for Wood, J: *of Composite Materials,* Vol. 18, pg. 216-226.

15. Attaway, S. W. (1988) A Local Isotropic/Global Orthotropic Finite Element Technique for Modeling the Crush of Wood, SAND88- 1449, Sandia National Laboratories, pas 45.

16. Norris, C. B. (1950) Strength of Orthotropic Materials Subject to Combined Stresses. USDA Forest Service, Forest products Laboratory, Report No. 1816.

17. Bodig, J. and Goodman, J.R. (1973) Prediction of Elastic Parameters for Wood. *Wood Sci.,* Vol. 5, No. 4, pp. 249-264.

18. Megraw, R.A., (1985) *Wood Quality Factors in Loblolly Pine,* TAPPI Press, Atlanta, GA

19. Cramer, S.M., Hermanson, J.C. and McMurtry, W.M. (In press) Crush Performance of Redwood for Developing Design Procedures for Impact Limiters. Proceedings of PATRAM '95, Packaging and Transportation of Radioactive Materials.

20. Strickler, M. D. and Pellerin, R.F. (1973) Rate of Loading Effect on Strength of Wood Parallel to Grain. *Forest Products Journal,* Vol. 23, No. 10, pp. 34-36.

21. DeBonis, A.L., Woeste, F.E., and McLain, T.E. (1980) Rate of Loading Influence on Southern Pine 2 by 4's in Bending. *Forest Products Journal,* Vol. 30, No. 11, pp. 34-37.

22. Bender, D. A., Taylor, S. E., and Swinnea, J. W. (1988) Load Rate Adjustment for Tensile Proof Testing of Southern Pine 2 by 10's. *Forest Products Journal,* Vol. 38, No. 6, pp. 26-30.

23. Gerhards, C.C. (1977) Effect of Duration and rate of Loading on Strength of Wood and Wood-Based Materials. Res. Pap. FPL 283. USDA Forest Service, Forest Products Lab., Madison, Wis.

24. Liska, J. A.. (1950) Effect of Rapid Loading on the Compressive and Flexural Strength of Wood. USDA Forest Service, Forest Products Laboratory, Report No.R1767.

25. Reid, S. R., Peng, C. and Reddy, T. Y. (1989) Dynamic Uniaxial Crushing and Penetration of Wood. *Proceedings of the Int. Conf. Mech. Prop. Materials at High Rates of Strain.* IOP Publishing, Oxford, England.

26. Hoadley, B. (1990). *Identifying wood.* The Taunton Press. Newtown, CT.

APPENDIX

Test No.	Specimen ID	Face Orientation	Target Grain Angle, degrees	Date Tested	Moisture Content	Specific Gravity	Rings per Inch	Grain Angle Measured	Nominal Crush Stress, psi
AMBIENT CONDITION TESTS									
1	C642 0		0	18-Apr-92	13.60%	0.29	2.80	0.10	3660
2	C643 0		0	25-Apr-92	12.70%	0.29	2.80	1.40	3831
3	C644 0		0	20-May-92	12.60%	0.30	2.80	1.20	3639
4	C346 0		0	03-lun-92	13.60%	0.40	20.80	1.10	5385
5	C611 0		0	04-lun-92	13.80%	0.30	2.30	1.30	3430
6	C535	R	5	24-Apr-92	12.90%	0.30	6.S	5.90	4164
7	C311	R	5	20-May-92	12.70%	0.38	18.50	4.80	4426
8	C815	R	5	21 -May-92	13.00%	0.40	23.80	5.60	4670
9	C813	R	5	22-May-92	13.50%	0.39	23.80	5.60	4580
10	C843	R	5	04-Jun-92	14.196	0.41	21.00	5.80	4472
11	C812	T	5	21-Apr-92	14.00%	0.38	23.80	3.60	4899
12	C321	T	5	25-Apr-92	13.70%	0.38	19.30	6.00	4771
13	C138	T	5	04-Jun-92	13.40%	0.34	10.50	4.40	4246
14	C746	T	5	28-Sep-92	13.90%	0.41	18.00	6.30	4845
15	C316	R	10	19-May-92	13.30%	0.38	17.5	9.60	4723
16	C816	R	10	21-May-92	13.20%	0.39	23.80	11.50	4913
17	C719	R	10	22-MaY-92	13.40%	0.45	19.00	9.20	5155
18	C713	R	10	22-May-92	13.40%	0.45	22.50	9.00	5358
19	C817	T	10	24-Apr-92	13.80%	0.41	23.80	11.10	5169
20	C534	T	10	25-Apr-92	13.10%	0.29	6.50	8.00	3681
21	C342	T	10	02-Jun-92	13.30%	0.39	19.00	8.80	4951
22	C715	T	10	03-Jun-92	14.20%	0.44	22.50	9.60	4853
23	C831	T	10	03-Jun-92	13.90%	0.43	17.30	11.80	4882
24	C718	R	30	01 -Jun-92	13.10%	0.44	19.00	27.80	3432
25	C345	R	30	02-Jun-92	13.20%	0.41	16.50	28.60	2888
26	C613	R	30	03-Jun-92	13.50%	0.33	2.50	28.10	2777
27	C533	R	30	04-Jun-92	13.20%	0.29	6.50	26.40	2810
28	C312	T	30	20-May-92	12.50%	0.38	18.50	27.50	3416
29	C536	T	30	22-May-92	13.20%	0.31	6.50	26.80	2897
30	C? 11	T	30	02-Jun-92	13.30%	0.43	No data	27.60	4281
31	C344	T	30	02-Jun-92	13.70%	0.39	16.50	28.00	3718
32	C314	T	30	02-Jun-92	12.60%	0.38	No data	26.00	3671
33	C532	R	90	21 -Apr-92	12.90%	0.30	6.50	89.30	850
34	C645	R	90	25-Apr-92	13.40%	0.30	2.50	89.40	1097
35	C135	R	90	21-May-92	13.10%	0.36	11.00	86.00	965
36	C641	T	90	01 -Jun-92	12.60%	0.30	2.50	86.90	845

Test No.	Specimen ID	Face Orientation	Target Grain Angle, degrees	Date Tested	Moisture Content	Specific Gravity	Rings per Inch	Grain Angle Measured	Nominal Crush Stress, psi
HOT CONDITIONS TEST									
1	C614		0	19-Jul-92	5.40%	0.32	2.6	1.6	4074
2	C143		0	21-Jul-92	4.00%	0.33	11.80	1.80	5605
3	C531 A		0	23-Jul-92	2.30%	0.31	7.30	0.90	5428
4	C846		0	03-Aug-92	3.30%	0.42	20.00	0.80	6749
5	C749A		0	03-Aug-92	3.70%	0.42	16.80	1.80	6559
6	C844	R	5	21-Jul-92	4.30%	0.42	22.50	5.20	5817
7	C735	R	5	21-Jul-92	3.70%	0.40	17.00	4.90	5850
8	C546	R	5	28-Jul-92	2.30%	0.32	8.50	5.40	5327
9	C 147	R	5	31-lul-92	2.90%	0.34	12.50	4.00	4869
10	C145	T	5	18-lul-92	5.10%	0.34	13.00	4.70	5119
11	C732	T	5	18-Jul-92	5.50%	0.39	18.00	4.60	5363
12	C541	T	5	08-Au -92	3.50%	0.30	7.30	3.90	4971
13	C 149	T	5	08-Aug-92	4.90%	0.34	12.00	4.20	5231
14	C736	R	10	17-lul-92	1.90%	0.41	17.00	10.20	4920
15	C814	R	10	28-Jul-92	2.30%	0.41	23.80	9.00	5731
16	C320	R	10	11-Au -92	8.70%	0.40	193	10.30	4466
17	C318	R	10	11-Au -92	8.40%	0.40	19.80	8.90	4666
18	C 144	T	10	22-Jul-92	3.20%	0.34	13.00	9.60	5278
19	C716	T	10	27-Jul-92	4.90%	0.45	17.50	8.20	6665
20	C146	T	10	31-Jul-92	6.10%	0.33	11.00	11.20	4250
21	C733	T	10	04-Aug-92	7.50%	0.40	18.00	7.50	5327
22	C739	R	30	18-Jul-92	5.70%	0.41	18.50	28.10	4129
23	C142	R	30	31-Jul-92	4.40%	0.34	11.30	31.40	3562
24	C743	R	30	31 -Jul-92	8.60%	0.43	13.50	29.20	3321
25	C745	R	30	11-Aug-92	9.70%	0.41	14.50	29.10	3197
26	C 137	T	30	31 -Jul-92	5.20%	0.36	10.80	24.50	4266
27	C749	T	30	10-Aug-92	9.00%	0.41	17.00	30.90	3709
28	C548	T	30	11-Aug-92	8.00%	0.31	8.00	29.60	2875
29	C545	T	30	11 -Aug-92	7.10%	0.32	8.00	29.40	3083
31	C542	R	90	22-Jul-92	2.40%	0.30	7.30	89.00	885
31	C 139	R	90	04-Aug-92	6.50%	0.35	10.80	88.60	1009
32	C 148	T	90	17-Jul-92	1.70%	0.34	12.30	88.50	1111
33	C348	T	90	27-Jul-92	3.80%	0.44	18.30	88.20	1151

Test No.	Specimen ID	Face Orientation	Target Grain Angle, degrees	Date Tested	Moisture Content	Specific Gravity	Rings per Inch	Grain Angle Measured	Nominal Crush Stress, psi
COLD CONDITION TEST									
1	C611 A		0	02-Dec-92	13.50%	0.30	2.30	0.20	5178
2	C842		0	06-Dec-92	13.70%	0.41	21.50	0.60	7766
3	C133		0	08-Dec-92	12.50%	0.35	11.00	0.60	7000
4	C744		0	09-Dec-92	14.00%	0.42	17.30	1.50	7074
5	C 117	R	5	09-Dec-92	15.70%	0.34	12.00	5.50	5959
6	C748	R	5	04-Dec-92	14.20%	0.41	17.00	4.50	6394
7	C717	R	5	05-Dec-92	13.90%	0.44	20.80	4.60	7627
8	C136	R	5	09-Dec-92	12.60%	0.36	11.50	4.80	6933
9	C845	T	5	02-Dec-92	14.30%	0.41	22.50	6.40	7241
10	C544	T	5	03-Dec-92	13.10%	0.30	7.50	4.20	5663
11	C738	T	5	05-Dec-92	13.80%	0.40	17.00	4.00	6821
12	C131	T	5	07-Dec-92	12.40%	0.35	10.00	7.30	6474
13	C521	R	10	11-Dec-92	12.60%	0.32	7.00	9.40	6163
14	C742	R	10	05-Dec-92	14.10%	0.43	16.00	10.50	7009
15	C714	R	10	09-Dec-92	14.00%	0.45	21.00	10.70	8052
16	C115	R	10	10-Dec-92	15.40%	0.34	13.00	9.30	5949
17	C741	T	10	05-Dec-92	13.90%	0.43	17.00	12.00	6827
18	C847	R	10	06-Dec-92	13.80%	0.41	20.50	9.40	7110
19	C341	T	10	07-Dec-92	13.10%	0.39	20.00	10.30	7306
20	C737	T	10	08-Dec-92	13.70%	0.39	16.50	10.30	6602
21	C525	R	30	11-Dec-92	12.90%	0.32	6.90	28.20	4365
22	C118	R	30	11-Dec-92	15.30%	0.33	10.00	29.10	4174
23	C114	R	30	10-Dec-92	15.40%	0.33	10.00	30.00	3888
24	C113	R	30	10-Dec-92	15.70%	0.34	12.00	30.20	4104
25	C524	T	30	11-Dec-92	12.80%	0.31	8.40	30.60	4223
26	C523	T	30	11 -Dec-92	12.80%	0.31	7.50	31.30	4245
27	C134	T	30	06-Dec-92	12.70%	0.35	11.00	29.20	4795
28	C347	T	30	06-Dec-92	13.20%	0.40	19.50	253	5592
29	C543	R	90	05-Dec-92	12.60%	0.30	7.50	89.20	1059
30	C132	R	90	06-Dec-92	12.60%	0.35	11.00	88.70	1393
31	C616	R	90	09-Dec-92	13.30%	0.29	2.50	88.10	1400
32	C 112	T	90	11 -Dec-92	15.20%	0.34	11.30	87.10	1350
33	C531	T	90	03-Dec-92	13.00%	0.29	7.20	88.50	1104
34	C615	T	90	09-Dec-92	13.00%	0.30	2.30	89.00	1251

DISTRIBUTION

1 Mr. Ashok Kapoor
U.S. Department of Energy
Office of Transportation, Emergency Management, and Analytical Services
EM-70, Cloverleaf Building
19901 Germantown Road
Germantown, MD 2087-1290

3 U.S. Department of Energy
Office of Transportation, Emergency Management, and Analytical Services
EM-76, Cloverleaf Building
19901 Germantown Road
Germantown, MD 2087-1290

Attn: Mike Keane
Mike Controy
Rich Brancato

2 U.S. Department of Energy
Albuquerque Field Office
Mail Stop 1396
P.O. Box 5400
Albuquerque, NM 87185-1396

Attn: P. Grace
P. Dickman

1 Mr. William Lake
U.S. Department of Energy
RW-431
Forrestal Building
1000 Independence Avenue SW
Washington, DC 20585

6 University of Wisconsin—Madison
Department of Civil Engineering
Madison, WI 53706

Attn: Steven M. Cramer (3)
J. C. Hermanson (3)

1 Richard Rawl
Wagramerstasse 5
P.O. 100
A-1400 Vienna, Austria

1 G. Field
MS G2-02
Westinghouse Hanford Company
P. O. Box 1970
Richland, WA 99352

1 Ron Pope
MS 6495
Oak Ridge National Laboratory
P.O. Box 2008
Oak Ridge, TN 37831-6495

1 MS 0715 R. E. Luna, 6610
10 MS 0715 TTC Library, 6610
1 MS 0716 C. Olson, 6643 actg.
1 MS 0716 P. E. McConnell, 6643
1 MS 0717 G. F. Hohnstreiter, 6642
10 MS 0717 W. M. McMurtry, 6642
1 MS 0717 D. J. Ammerman, 6642
1 MS 0717 M. E. McAllaster, 6642
1 MS 0717 J. D. Pierce, 6642
1 MS 0717 J. K. Rader, 6642
1 MS 0718 H. R. Yoshimura, 6641
1 MS 0724 J. B. Woodard, 6000
1 MS 0726 J. K. Rice, 6600
2 MS 0100 Document Processing, 7613-2, For DOE/OSTI
1 MS 0619 Print Media, 12615
5 MS 0899 Technical Library, 4414
1 MS 9111 Central Tech Files, 8523-2